IV　研究成果の刊行に関する一覧表

雑誌　（主なものを７つ選んで掲載）

発表者氏名	論文タイトル名	発表誌名	巻号	ページ	出版年
Soga M, Ishitsuka Y, Hamasaki M, Yoneda K, Furuya H, Matsuo M, Ihn H, Fusaki N, Nakamura K, Nakagata N, Endo F, Irie T, Era T.	HPGCD outperforms HPBCD as a potential treatment for Niemann-Pick disease type C during disease modeling with iPS cells.	Stem Cells	33	1075-1088	2015
Shahjalal HM, Shiraki N, Sakano D, Kikawa H, Ogaki S, Baba H, Kume K., Kume S.	Generation of insulin-producing beta-like cells from human iPS cells in a defined and completely Xeno-free culture system.	Journal of Molecular Cell Biology	6	394-408	2014
Matsuo M, Shraishi K, Wada K, Ishitsuka Y, Doi H, Iimori Y, Mizoguchi T, Eto J, Mochinaga S, Arima H, Irie T	Effects of intracerebroventricular administration of 2-hydroxypropyl-β-cyclodextrin in a patient with Niemann-Pick Type	Molecular Genetics and Metabolism Reports.	1	391-400	2014
Murray A, Letourneau A, Canzonetta C, Stathaki E, Gimelli S, Sloan-Bena F, Abrehart R, Goh P, Lim S, Baldo C, Dagna-Bricarelli F, Hannan S, Mortensen M, Ballard D, Syndercombe Court D, Fusaki N, Hasegawa M, Smart TG, Bishop C, Antonarakis SE, Groet J, Nizetic D.	Isogenic Induced Pluripotent Stem Cell Lines from an Adult with Mosaic Down Syndrome Model Accelerated neuronal Ageing and Neurodegeneration.	Stem Cells	Feb.19	[Epub ahead of print]	2015

発表者氏名	論文タイトル名	発表誌名	巻号	ページ	出版年
Kadohisa M, Matsumoto S, Sawada H, Honda M, Murokawa T, Hayashida S, Ohya Y, Lee KJ, Yamamoto H, Mitsubuchi H, Endo F, Inomata Y.	Living donor liver transplantation from a heterozygous parent for classical maple syrup urine disease.	Pediatric Transplantation	19	E66-E69.	2015
Maeda Y, Motoyama K, Higashi T, Horikoshi Y, Takeo T, Nakagata N, Kurauchi Y, Katsuk H, Ishitsuka Y, Kondo Y, Irie T, Era T, Furuya H, Arima H.	Effects of Cyclodextrins on GM1-gangliosides in Fibroblasts from GM1-gangliosidosis Patients	Journal of Pharmacy and Pharmacology			*in press*
Inoue T, Kulkeaw K, Muennu K, Tanaka Y, Nakanishi Y, Sugiyama D.	Herbal drug ninjin'yoeito accelerates myelopoiesis but not erythropoiesis in vitro.	Genes to Cells	19	432-440	2014

V　研究成果の刊行物・別刷

STEM CELLS

EMBRYONIC STEM CELLS/INDUCED PLURIPOTENT STEM CELLS

HPGCD Outperforms HPBCD as a Potential Treatment for Niemann-Pick Disease Type C During Disease Modeling with iPS Cells

MINAMI SOGA,[a] YOICHI ISHITSUKA,[b] MAKOTO HAMASAKI,[a] KAORI YONEDA,[c] HIROKAZU FURUYA,[d] MUNEAKI MATSUO,[e] HIRONOBU IHN,[f] NOEMI FUSAKI,[g,h] KIMITOSHI NAKAMURA,[c] NAOMI NAKAGATA,[i] FUMIO ENDO,[c] TETSUMI IRIE,[b] TAKUMI ERA[a]

[a]Department of Cell Modulation, Institute of Molecular Embryology and Genetics; [b]Department of Clinical Chemistry and Informatics, Graduate School of Pharmaceutical Sciences; [c]Department of Pediatrics, Graduate School of Medical Sciences, and [f]Department of Dermatology and Plastic Surgery, Faculty of Life Sciences; [i]Division of Reproductive Engineering, Center for Animal Resources and Development, Kumamoto University, Kumamoto, Japan; [d]Department of Neurology, Neuro-uscular Center, National Omuta Hospital, Omuta, Fukuoka, Japan; [e]Department of Pediatrics, Saga University, Faculty of Medicine, Saga, Japan; [g]DNAVEC Corporation, 6 Ookubo, Tsukuba, Ibaragi, Japan; [h]Precursory Research for Embryonic Science and Technology (PRESTO), Japan Science and Technology Agency (JST), Kawaguchi, Saitama, Japan

Correspondence: Takumi Era, Ph.D., M.D., Department of Cell Modulation, Institute of Molecular Embryology and Genetics, Kumamoto University, 2-2-1 Honjo, Chuo-ku, Kumamoto 860-0811, Japan. Telephone: 81-96-373-6589; Fax: 81–96-373-6590; e-mail: tera@kumamoto-u.ac.jp or Tetsumi Irie, Ph.D., Department of Clinical Chemistry and Informatics, Graduate School of Pharmaceutical Sciences, Kumamoto University, 5-1 Oe-honmachi, Chuo-ku, Kumamoto 862–0973, Japan. Telephone: 81-96-371-4552; Fax: 81-96-371-4552; e-mail: tirie@gpo.kumamoto-u.ac.jp.

Received June 13, 2014; accepted for publication October 31, 2014; first published online in STEM CELLS EXPRESS December 17, 2014.

1066-5099/2014/$30.00/0

http://dx.doi.org/10.1002/stem.1917

Key Words. Induced pluripotent stem cells • Transgene-free • Niemann-Pick disease type C • Experimental models

ABSTRACT

Niemann-Pick disease type C (NPC) is a lysosomal storage disease characterized by abnormal accumulation of free cholesterol and glycolipids. Here, we established induced pluripotent stem cell (iPSC) lines from NPC patients. Hepatocyte-like cells (HLCs) and neural progenitors derived from the iPSC lines accumulated cholesterol and displayed impaired autophagy and ATP production. A molecular signature related to lipid metabolism was also impaired in the NPC-iPSC-derived HLCs. These findings indicate that iPSC-derived cells can phenocopy human NPC. We also newly found that 2-hydroxypropyl-γ-cyclodextrin (HPGCD) could reduce the cholesterol accumulation and restore the functional and molecular abnormalities in the NPC patient-derived cells, and do so more effectively than 2-hydroxypropyl-β-cyclodextrin treatment. In addition, NPC model mice showed an improved liver status and prolonged survival with HPGCDs. Thus, iPSC lines derived from patient cells are powerful tools to study cellular models of NPC, and HPGCD is a potential new drug candidate for future treatment of this disease. STEM CELLS *2015;33:1075–1088*

INTRODUCTION

Induced pluripotent stem cells (iPSCs), which are artificially produced from human somatic cells, can be further induced to undergo sustained, unlimited growth, and exhibit multipotency (i.e., the ability to give rise to various cell types in vitro) [1, 2]. Because of these features, iPSCs are a potential source for cell therapy applications in clinical medicine. The process of iPSC generation, known as reprogramming, is triggered by the expression of four transcription factors, Oct3/4, Sox2, Klf4, and c-Myc, which are the same core factors underlying pluripotency in other pluripotent stem cells such as embryonic stem cells (ESCs) [3–5]. In particular, many procedures have now been reported to easily generate iPSCs from human fibroblasts and peripheral blood cells [6, 7].

Numerous iPSC lines derived from the somatic cells of patients harboring pathogenic mutations have been established and shown to phenocopy the disease [8–13]. These studies clearly demonstrated that disease-derived iPSC lines represent a powerful tool not only for cell therapy, but also for biomedical research and drug development [14, 15]. In particular, biomaterial samples obtained from patients with intractable diseases are indispensable for studying the underlying molecular mechanisms and developing new therapeutic agents. However, because the number and size of samples available from such patients are usually limited, disease-derived iPSCs are expected to be useful mainly as a replacement or supplemental source of biomaterials for developing new therapies.

Niemann-Pick disease type C (NPC) is a hereditary intractable disease associated with mutations in the lipid transporter genes, *NPC1* and *NPC2* [16, 17]. NPC1 helps to transport cholesterol between lysosomes and endoplasmic reticulum (ER) in cooperation with NPC2. Mutations in the *NPC1* and *NPC2* genes disrupt this transporting system, resulting in the accumulation of free cholesterol and glycolipids in lysosomes [18]. NPC patients suffer from liver and neurological dysfunctions and eventually die due to respiratory and hepatic failure [18]. Miglustat is a lipogenesis inhibitor indicated for NPC; however, its effect is so limited that patients eagerly await new advances in drug development for NPC therapy [19].

Our work aims to generate iPSC lines from patients with NPC to establish a disease model mirroring the cellular phenotype of NPC, and then use this model to screen drug candidates. To generate the iPSC lines from NPC patients safely and efficiently, we took advantage of the SeV vector that does not integrate into host genomes and can easily provide transgene-free iPSC lines. In this study, we generated iPSC lines from NPC skin fibroblasts, and found that subsequently derived hepatocyte-like cells (HLCs) and neural progenitors accumulate free cholesterol and exhibit functional defects. Using this system, we tested three types of cyclodextrin drugs for their ability to reduce the cholesterol accumulation. Interestingly, in addition to 2-hydroxypropyl-β-cyclodextrin (HPBCD), we newly found that 2-hydroxypropyl-γ-cyclodextrin (HPGCD) could remove the free cholesterol accumulated in NPC-derived HLCs and neural progenitors and restore the functionality of the HLCs. Moreover, liver dysfunction and cholesterol accumulation in NPC model mice were markedly improved with the HPGCD treatment. Dose-loading tests also showed that HPGCD is much safer than HPBCD. Our findings confirm the potential value of NPC-derived iPSC lines for studying cellular models of disease and highlight HPGCD as a future drug candidate for NPC.

Materials and Methods

iPSC Generation

iPSCs were generated from human skin-derived fibroblasts as described previously [20]. Briefly, 5×10^5 cells of human fibroblast cells per well of six-well plate were seeded 1 day before infection and then were infected with Sendai virus (SeV) vectors at 10 multiplicity of infection. After 7 days of culturing for fibroblasts, the infected cells were harvested by trypsin and replated at 5×10^4 cells per 60-mm dish on mitomycin C-treated mouse embryonic fibroblast feeder cells. From 18 to 25 days after infection, colonies were picked and recultured in human iPSC medium. To remove Sendai virus, the temperature of culture was shifted from 37°C to 38°C for 3 days at passage 1 or 2 of the iPSCs. Other materials and methods are described in Supporting Information Materials and Methods.

Results

Establishment of Disease-Derived iPSC Lines

To establish a cellular model of NPC, we attempted to generate iPSC lines from skin fibroblasts of two patients carrying different *NPC1* mutations. The efficiency of iPSC generation from these patients was similar to that from healthy volunteers, suggesting that *NPC1* mutations do not affect the efficiency of cell reprogramming (Supporting Information Fig. S1A). The NPC fibroblast-derived iPSCs exhibited ESC-like morphology and expressed a set of pluripotent markers (Fig. 1A; Supporting Information Fig. S1B, S1C). The nested PCR that can detect a single positive cell among 1 million cells confirmed a free of SeV contamination (Supporting Information Fig. S1B, S1D). We then investigated the differentiation potential of our NPC-derived iPSCs by evaluating teratoma formation. Histological analysis revealed that the teratomas analyzed comprised descendants of all three germ cell layers such as cuboidal epithelia, melanin pigment-containing cells, cartilage, muscle, and various glandular structures (Supporting Information Fig. S1E). The NPC iPSC lines had a normal karyotype, 46XY and 46XX, and mutations in the *NPC1* gene were confirmed by DNA sequencing (Supporting Information Fig. S1F, S1G). Thus, the NPC-derived iPSCs fulfilled the criteria for iPSC lines.

Morphological and Functional Analyses of NPC-Derived iPSC Lines

Liver enlargement is a major symptom of NPC patients, and those with severe forms of the disease suffer from liver dysfunction and failure [18]. To investigate the effect of Npc1 deficiency on the hepatocytic lineage, we differentiated NPC-derived iPSC lines into HLCs expressing albumin. We previously demonstrated that treatment with Activin A selectively induces the differentiation of mouse ESCs into definitive endoderm cells and HLCs, and that an endodermal surface marker, Cxcr4, could be used to detect endodermal differentiation [21, 22]. Thus, in this study, we similarly directed the iPSC lines into endodermal and hepatic lineages (Supporting Information Fig. S2A). On day 18 of differentiation, the HLCs expressed α-fetoprotein (~65% of total cells), albumin (~80% of total cells), and other hepatic markers (Supporting Information Fig. S2B, S2C); they also absorbed indocyanine green (ICG) and stored glycogen (Supporting Information Fig. S3A). The generation rate of definitive endoderm-like cells, calculated as the percentage of Cxcr4-positive cells (Supporting Information Fig. S3B), and the efficiency of hepatic differentiation, calculated from the percentage of albumin-positive cells and the marker expressions (Fig. 1B; Supporting Information Fig. S2C), were similar between the normal cell- and NPC-derived iPSC lines. In contrast, the NPC-derived HLCs were larger than the control HLCs (Fig. 1C). In NPC patients, defective transportation of cholesterol from lysosomes to ER results in the accumulation of free cholesterol in lysosomes [18]. Therefore, we used filipin staining, which specifically detects free cholesterol in cells, to assess the level of cholesterol accumulation. We observed negligible numbers of positively stained cells in the control HLCs derived from healthy volunteers, whereas the NPC-derived HLCs showed extreme levels of cholesterol accumulation (Fig. 1D), suggesting that these cells mirror the cellular phenotype of NPC.

Next, we investigated the various functions of HLCs generated from normal and NPC-derived iPSC lines. We could not detect any differences in terms of ICG uptake or release, glycogen storage, albumin production, urea secretion, or ammonia removal, all of which are indicative of hepatocyte function (Supporting Information Fig. S3A, S3C–S3E). The ATP levels in NPC-HLCs were significantly lower than those in control HLCs (Fig. 1E), although apoptosis in the NPC-HLCs was not exacerbated compared to that in the controls (Supporting Information Fig. S3F, S3G). To investigate the membrane potential of mitochondria, we used the specific MitoTracker staining reagents, JC-1 and CMXRos [23, 24]. JC-1 concentrates in the mitochondria and aggregates at normal mitochondrial membrane potentials, resulting in a high red/green fluorescence intensity ratio. Reduced mitochondrial membrane potential affects the aggregation of JC-1, resulting in a decreased red/green fluorescence intensity ratio. In addition, CMXRos

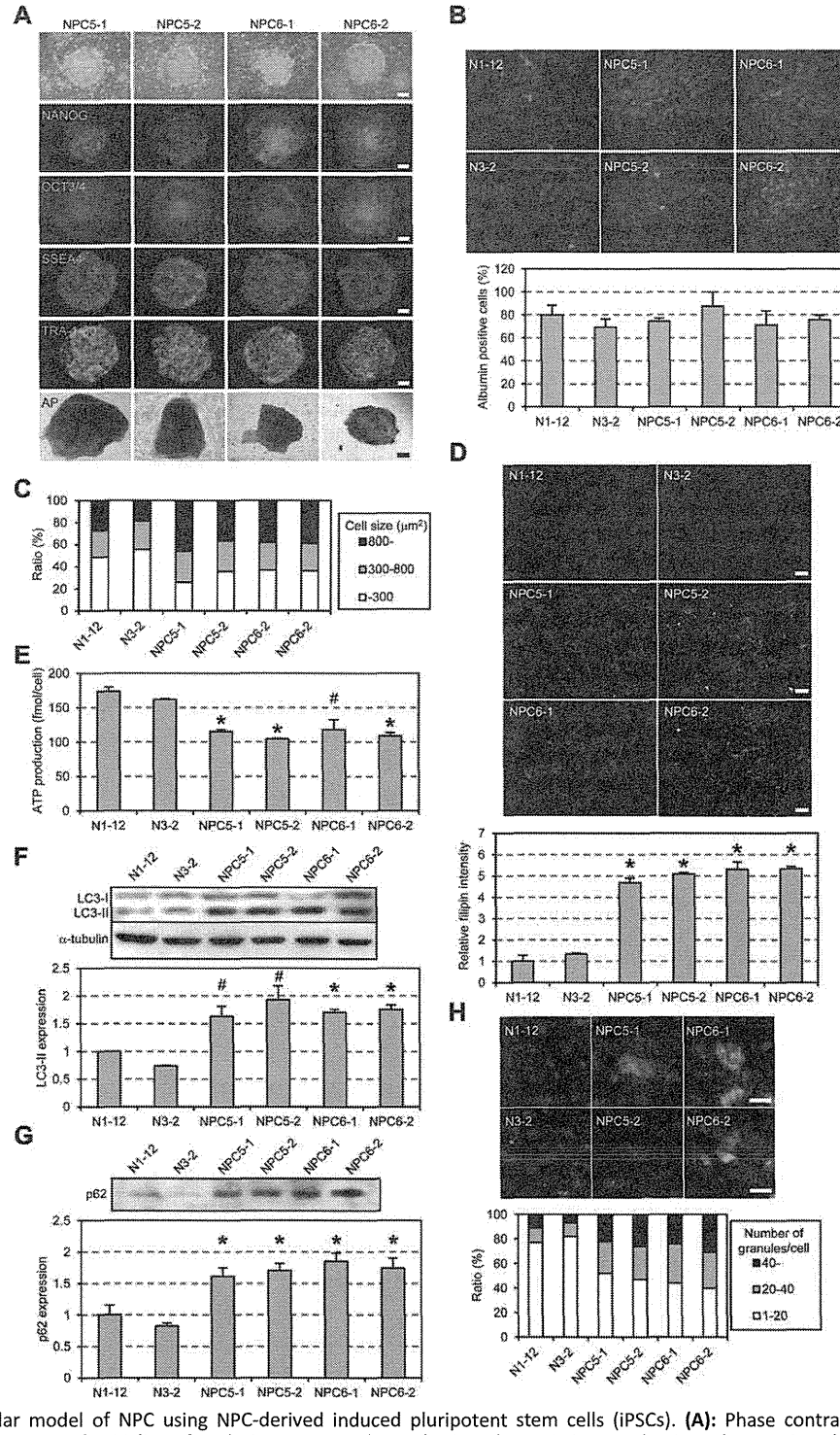

Figure 1. A cellular model of NPC using NPC-derived induced pluripotent stem cells (iPSCs). **(A):** Phase contrast images, immunofluorescence, and AP staining of iPSC lines for pluripotency markers. The iPSC lines NPC5-1 and −2, and NPC6-1 and −2, were derived from the NPC patients, NPC5 and NPC6, respectively. Scale bars = 200 μm. **(B):** Albumin expression in normal and NPC-derived hepatocyte-like cells (HLCs). Representative images of immunostaining for albumin (green) and propidium iodide staining of nuclei (blue) are shown in the upper panels. The bar graph in the lower panel shows the means ± SD of three independent experiments. The proportion of albumin-positive cells in differentiated NPC-derived iPSC lines was similar to that in the normal control. Scale bars = 100 μm. **(C):** Cell size of HLCs. The cell size of albumin-positive cells in Figure 1B was calculated using IN CELL ANAYZER 6000 (GE Healthcare). The NPC-derived HLCs were larger than normal HLCs. **(D):** Cholesterol accumulation in HLCs derived from NPC-iPSC lines. Free cholesterol was examined by filipin staining (upper image), and the relative intensity was calculated relative to the normal iPSC line, N1–12 (lower graph). Data are means ± SD of three independent experiments. NPC-derived HLCs showed a marked and significant accumulation of free cholesterol compared with HLCs derived from the normal iPSC lines, N1–12 and N3-2. *, $p < .01$, indicated NPC-iPSC line versus normal iPSC lines, Student's *t* test. Scale bars = 100 μm. **(E):** ATP levels in HLCs derived from iPSC lines. Experiments were conducted in triplicate (mean ± SD). The ATP levels were significantly lower in NPC-derived HLCs than in normal controls. *, $p < .01$; #, $p < .05$, indicated NPC-iPSC line versus normal iPSC lines, Student's *t* test. **(F):** Autophagy was upregulated and the protein levels of LC3-II were significantly elevated in NPC-derived HLCs. *, $p < .01$; #, $p < .05$, indicated NPC-iPSC lines versus normal iPSC lines, N1–12, and N3-2, Student's *t* test. The expression level was normalized to the expression of α-tubulin in each iPSC line. **(G):** Impairment of autophagic flux in NPC-derived HLCs. The insoluble form of p62 was enhanced in NPC-derived HLCs compared with that in normal HLCs. **(H):** Immunofluorescence staining for p62. Abnormal aggregation of p62 was strongly present in NPC-derived HLCs (green, upper panel). The aggregated granules were counted and the results summarized in the lower graph. The proportion of cells carrying more than 40 granules was increased in NPC-derived HLCs compared to normal HLCs. Nuclear staining, Hoechst 33258 (blue); scale bars = 25 μm. Abbreviations: AP, alkaline phosphatase; NPC, Niemann-Pick disease type C.

accumulates in mitochondria at normal membrane potential. We could not detect any difference in staining patterns for JC-1 or CMXRos between normal and NPC-derived HLCs (Supporting Information Fig. S3H, S3I).

Cellular autophagy is impaired in lysosomal storage diseases [25], therefore we used two methods to monitor the autophagy pathway in our NPC-derived HLCs compared to controls. First, we examined expression of the autophagy marker, microtubule-associated protein 1 light chain 3 (LC3) (Fig. 1F) [26]. C-terminal processing of LC3 produces LC3-I, which is modified to LC3-II with the initiation of autophagosome formation. We also measured p62/SQSTM1 (p62) expression to assess autophagic flux (Fig. 1G, 1H) [27]. Because p62 binds to LC3 and is degraded upon fusion with the lysosome, impairment of autophagy flux results in the accumulation and aggregation of insoluble p62. The expression levels of LC3-II and insoluble p62 proteins were higher in NPC-HLCs than in normal HLCs (Fig. 1F, 1G). In addition, the NPC-derived HLCs showed excessive p62 aggregation compared with normal HLCs (Fig. 1H). These results suggested that autophagy is upregulated and autophagic flux is impaired in the NPC-derived HLCs.

Effect of Various Cyclodextrin Treatments on Cholesterol Accumulation and Restoration of Cellular Functions

A major aim of generating iPSCs from NPC patient cells is to develop an in vitro system for screening drug candidates. Our observation of extreme cholesterol accumulation in NPC iPSC-derived HLCs prompted us to examine the effect of various drug treatments on this process; specifically, we tested a series of 2-hydroxypropyl-cyclodextrins of different cavity sizes. 2-Hydroxypropyl-β-cyclodextrin (HPBCD) is effective for reducing cholesterol accumulation in *NPC1*-defective cells [28], and this was supported by our findings of significantly reduced cholesterol accumulation in NPC-HLCs with HPBCD treatment (Fig. 2A). Interestingly, 2-hydroxypropyl-α-cyclodextrin (HPACD) had no effect on cholesterol accumulation, while HPGCD reduced the cholesterol accumulation in NPC-HLCs to the same extent as HPBCD (Fig. 2A). The size of HLCs was also decreased by the treatments with HPBCD and HPGCD (Supporting Information Fig. S4A). Notably, low concentrations (100 μM) of HPBCD and HPGCD were ineffective for reducing cholesterol accumulation (Supporting Information Fig. S4B). The cholesterol accumulation does not appear before day 11 of the culture (Fig. 2B). In contrast, it is greatly and significantly enhanced on day 14, comparing to the control, and continuously increased up to day 22 during the hepatic differentiation. The 4-day treatments of HPBCD and HPGCD from day 18 to day 22 can significantly reduce the accumulation (Fig. 2B).

We next examined when during hepatic differentiation HPBCD and HPGCD are effective in reducing the NPC phenotype. By drug-treating our HLCs at various time points, we found that HPBCD and HPGCD effectively reduced cholesterol accumulation during the last 4 days (days 15–18) of hepatic differentiation (Fig. 2C). From days 15 to 18, differentiating HLCs express α-fetoprotein and albumin, and before day 15 the cells are intermediates between hepatic cells and iPSCs (Supporting Information Fig. S2B, S2C). These results therefore indicated that HPBCD and HPGCD could impede the cholesterol accumulation of NPC-derived cells at the hepatic cell stage in the in vitro iPSC cultures.

We next asked whether the cyclodextrin treatments could restore the abnormally low ATP levels and abnormal autophagy exhibited by the NPC-derived HLCs, and found that HPBCD and HPGCD treatment recovered both these functional abnormalities (Fig. 2D–2F; Supporting Information Fig. S4C).

NPC patients suffer from neural dysfunction [29], thus we examined whether neural cells derived from NPC-iPSCs also accumulate free cholesterol and if such a defect could be abrogated by HPGCD treatment. Neural progenitors expressing nestin were induced from healthy donor- and NPC-derived iPSCs and tested for marker expression during the neural differentiation. The expressions of the neural progenitor markers were gradually elevated in both normal and NPC-derived iPSC lines, whereas pluripotent markers such as Oct3/4 and Nanog were markedly decreased up to day 7 (Fig. 3A; Supporting Information Fig. S5A). These results suggest that the differentiation potential into neural progenitors in NPC-derived iPSC lines is almost equal to that in normal iPSC lines. However, the NPC-derived neural progenitors exhibited cholesterol accumulation that was significantly reduced with HPBCD and HPGCD treatments (Fig. 3B, 3C). Similar to NPC-derived HLCs, we found the low ATP levels and the abnormal autophagy which were restored with HPBCD and HPGCD treatments (Fig. 3D, 3E). HPBCD and HPGCD did not affect the levels of neural marker expression (Supporting Information Fig. S5B). These results indicated that both HLCs and neural cells derived from NPC-iPSCs are useful for evaluating drug candidates and that HPGCD, in addition to HPBCD, is a promising drug candidate for NPC treatment. Taken together, our data validate transgene-free iPSC lines as cellular models for NPC.

HPBCD and HPGCD Have a Different Effect on the Cholesterol Accumulation from Miglustat

Miglustat is used to treat NPC patients [30]. We next investigated the effect of Miglustat on the cholesterol accumulations in iPSC-derived neural progenitors and HLCs. Although HPGCD and HPBCD treatment could reduce the accumulations in both the cells, Miglustat could not at all remove the cholesterol accumulation from the cells with 4-day treatments (Fig. 4A). Similarly, neither ATP level nor abnormal autophagy were restored in both the cells with the Miglustat treatments (Fig. 4B, 4C; Supporting Information Fig. S6A, S6B). These results are reasonable because Miglustat is an enzyme inhibitor for glycosylceramide synthase, and suggest that the action mechanism of HPGCD and HPBCD is different from that of Miglustat [31]. We confirmed that Miglustat treatment could inhibit the glycosyl-ceramide synthesis in the iPSC-derived cells (Fig. 4D; Supporting Information Fig. S6C).

HPGCD Treatment Restores the Molecular Abnormalities More Effectively than HPBCD Treatment

We then used microarray analysis to further characterize the NPC-derived HLCs. A large number of genes were differentially expressed in each NPC-derived HLC line compared with healthy donor-derived HLCs, including 361 datasets of commonly downregulated and 362 datasets of commonly upregulated genes with a fold change >1.5 (Fig. 5A). To elucidate the functional significance of these changes in gene expression, we analyzed the commonly downregulated and

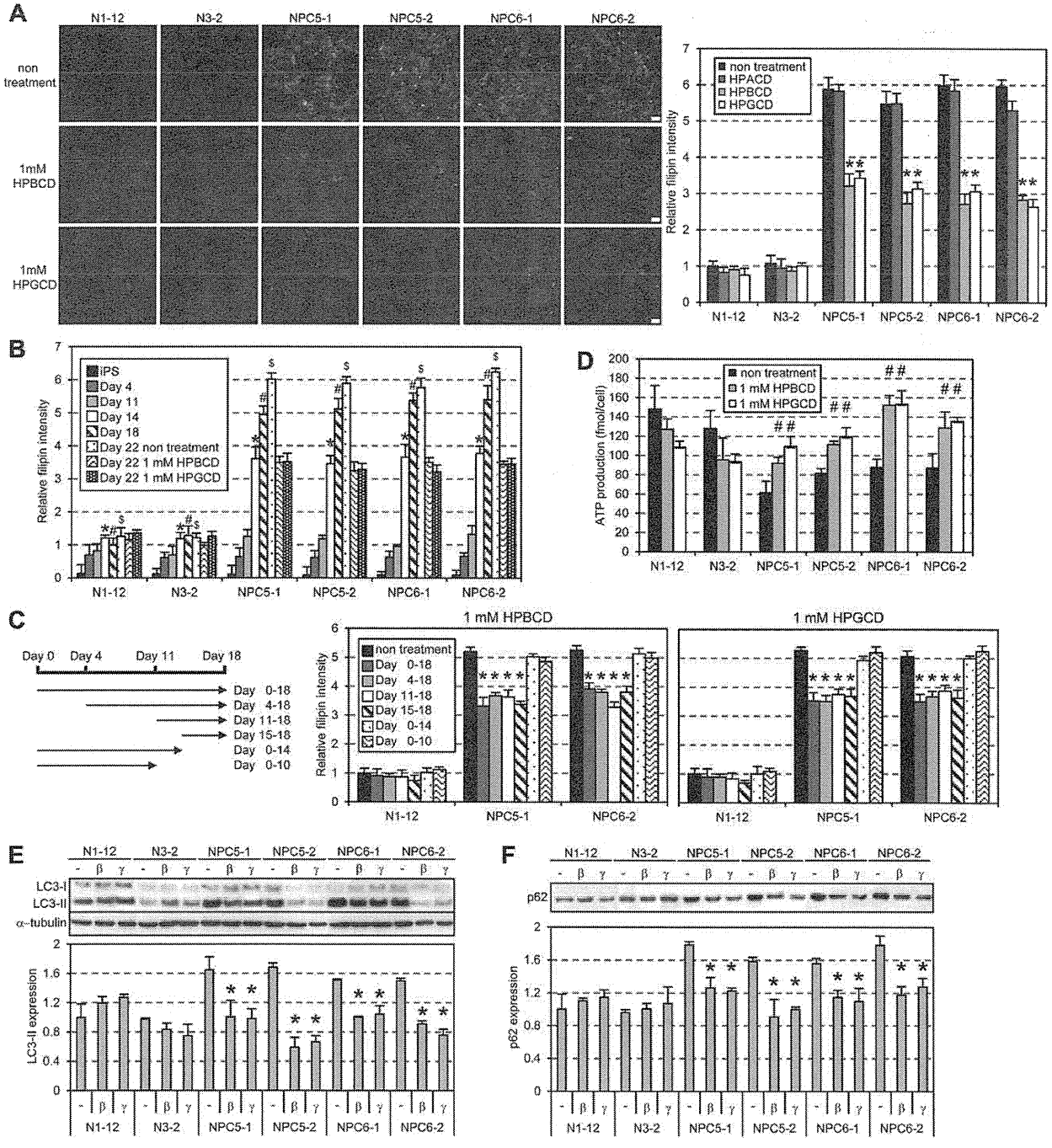

Figure 2. Effect of cyclodextrins on cholesterol accumulation in NPC-derived hepatocyte-like cells (HLCs). **(A):** Effect of a series of hydroxypropyl-cyclodextrins on the reduction of free cholesterol accumulation in NPC-derived HLCs. HLCs were cultured with 1 mM of the indicated hydroxypropyl-cyclodextrin for 4 days, filipin stained (left image), and analyzed with an IN Cell Analyzer (right graph, GE Healthcare). Data are means ± SD of three independent experiments. HPGCD and HPBCD, but not HPACD, significantly reduced free cholesterol accumulation in the NPC-derived HLCs. *, $p < .01$, nontreatment versus treatment of each NPC-derived HLC, Student's t test. Scale bars = 50 μm. **(B):** The free cholesterol accumulation during the hepatic differentiation. The filipin staining data were analyzed with an IN Cell Analyzer. The cells were treated with HPBCD and HPGCD from day 18 to day 22. Experiments were conducted in triplicate (mean ± SD). $^{*, \#, \$}$, $p < .01$, NPC clones versus normal clones, Student's t test. **(C):** Effects of HPBCD and HPGCD on the reduction of free cholesterol accumulation in NPC-derived induced pluripotent stem cell (iPSC) differentiation. The differentiated iPSCs were treated with 1 mM of HPBCD or HPGCD for the indicated times (left panel). The filipin staining data were analyzed with an IN Cell Analyzer (right graph). HPBCD and HPGCD treatments were effective at hepatic stages from day 15 to day 18 during in vitro iPSC differentiation. Experiments were conducted in triplicate (mean ± SD). *, $p < .01$, nontreatment versus treatment, Student's t test. **(D):** HPBCD and HPGCD treatments restored ATP levels of HLCs derived from NPC-iPSC lines. The levels were significantly recovered by treatments with HPBCD and HPGCD. HLCs were culture with 1 mM 2-hydroxypropyl-cyclodextrins (HPCDs) for 4 days. Data are means ± SD of three independent experiments. #, $p < .05$, nontreatment versus treatment, Student's t test. **(E):** HPCD treatments restored the abnormal induction of autophagy in NPC-derived HLCs. The expression level of LC3 was recovered to normal levels by treatments with HPBCD and HPGCD. β: Treatment with 1 mM HPBCD for 4 days, γ: 1 mM HPGCD treatment for 4 days. The expression level was normalized to α-tubulin expression in each iPSC line. **(F):** HPCD treatments restored the impairment of autophagic flux. HPBCD and HPGCD treatments reduced the amount of insoluble p62 in NPC-derived HLCs. β: Treatment with 1 mM HPBCD for 4 days, γ: 1 mM HPGCD treatment for 4 days. Abbreviations: HPACD, 2-hydroxypropyl-α-cyclodextrin; HPBCD, 2-hydroxypropyl-β-cyclodextrin; HPGCD, 2-hydroxypropyl-γ-cyclodextrin; NPC, Niemann-Pick disease type C.

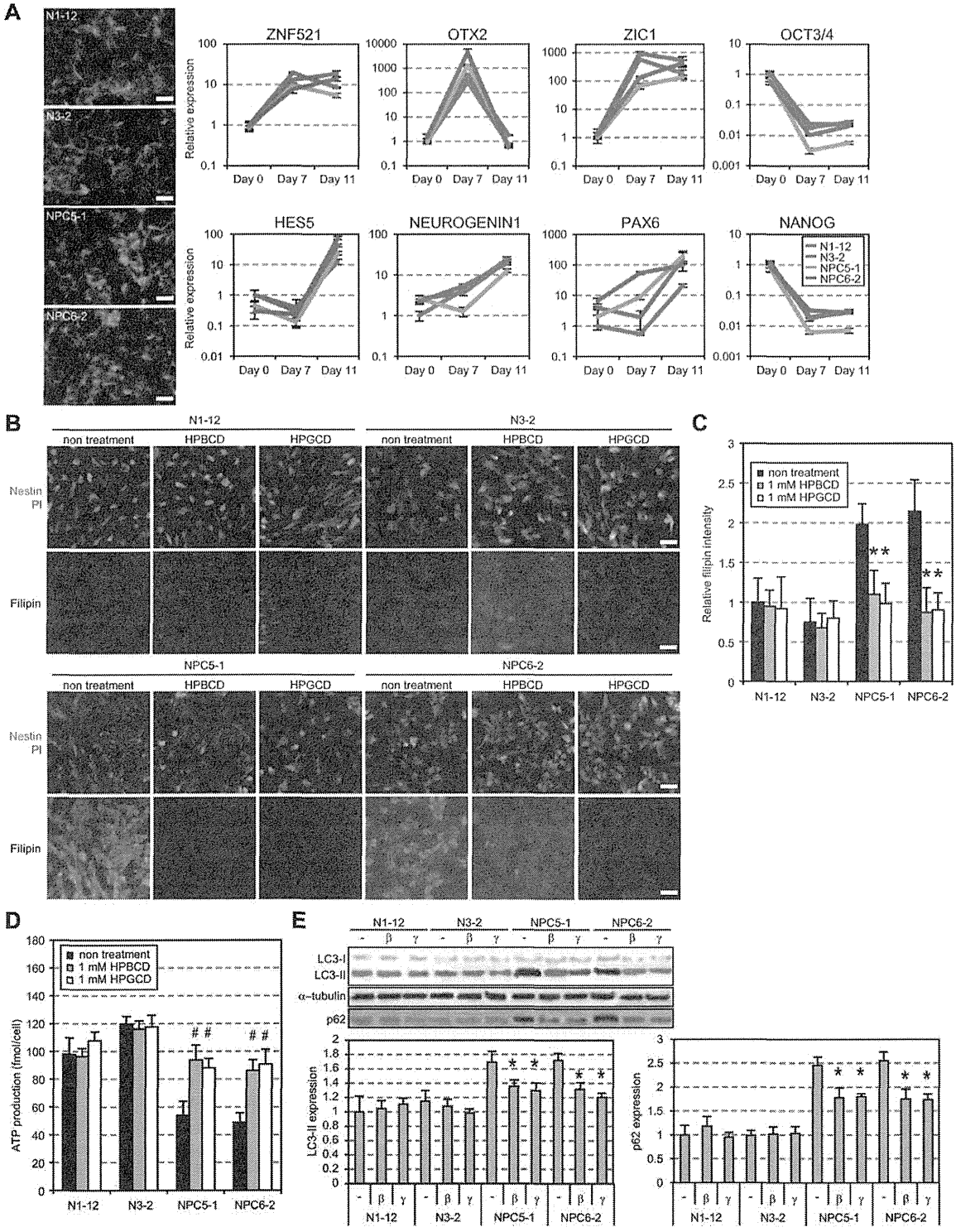

Figure 3. Effect of cyclodextrins on cholesterol accumulation in neural progenitors. **(A):** Marker expressions of neural progenitors derived from the induced pluripotent stem cell (iPSC) lines. The neural progenitors were induced from healthy donor- and NPC-derived iPSC lines. The cells showed expressed nestin (left panel, immunostaining) as well as other neural progenitor markers (right panel, qPCR). Scale bars = 50 μm. **(B, C):** Effect of HPBCD and HPGCD on the reduction of free cholesterol accumulation in NPC-derived neural progenitors. Neural progenitors were cultured with 1 mM of the indicated hydroxypropyl-cyclodextrin for 4 days, filipin, nestin and *PI* stained (B), and analyzed with an IN Cell Analyzer (C). Data are means ± SD of three independent experiments. HPGCD and HPBCD treatments significantly reduced free cholesterol accumulation in the nestin^{+} NPC-derived neural progenitors. *, $p < .01$, nontreatment versus treatment of each NPC-derived neural progenitors, Student's *t* test. Scale bars = 50 μm. **(D):** HPBCD and HPGCD treatments restored ATP levels of NPC-derived neural progenitors. The neural progenitors were culture with 1 mM 2-hydroxypropyl-cyclodextrins (HPCDs) for 4 days. Data are means ± SD of three independent experiments. #, $p < .05$, nontreatment versus treatment, Student's *t* test. **(E):** HPCD treatments restored the abnormal autophagy in NPC-derived neural progenitors. The expression levels of LC3 (upper and left lower panels) and p62 (upper and right lower panels) were decreased by treatments with HPBCD and HPGCD. β: Treatment with 1 mM HPBCD for 4 days, γ: 1 mM HPGCD treatment for 4 days. The expression level was normalized to α-tubulin expression in each iPSC line. Abbreviations: HPBCD, 2-hydroxypropyl-β-cyclodextrin; HPGCD, 2-hydroxypropyl-γ-cyclodextrin; NPC, Niemann-Pick disease type C; PI, propidium iodide.

upregulated genes identified using gene set enrichment analysis (GSEA). Analysis of the commonly downregulated genes revealed the following four molecular signatures to be significantly altered in NPC-derived HLCs compared to normal control cells: lipid metabolism, biosynthesis, cellular lipid metabolism, and cellular transport ($p < .05$; Fig. 5B). Among the 1,972 genes related to lipid metabolism, 10 genes were identified as downregulated by GSEA (HSD17B3, FSHB, ACACB, NAPEPLD, NR2F2, UGT2B15, PCYT1B, DGKE, APOC3, and CCL5) (Fig. 5C). Similarly, 46 and 34 genes related to biosynthesis and cellular transport, respectively, were identified as downregulated, and of these, 6 biosynthesis-related and 3 transport-related genes overlap with those related to lipid metabolism, while, 6 genes related to cellular lipid metabolism are absolutely included in the gene set related to lipid metabolism. Next, we investigated the effects of HPBCD and HPGCD on the expressions of genes included in the abnormal molecular signatures. The cluster analysis revealed that treatment of the cells with HPGCD shifted all the functionally related gene expression patterns closer to the normal patterns than treatment with HPBCD (Fig. 5C). Conversely, one molecular signature related to protein metabolism was identified among the commonly upregulated genes ($p < .05$; Fig. 5B); however, neither cyclodextrin treatment efficiently shifted this gene expression pattern toward that of the normal cells (Supporting Information Fig. S7A, Table S5). Taken together, the results indicated that lipid and protein metabolic processes are impaired in NPC-derived HLCs and that they are more effectively improved by HPGCD treatment than HPBCD treatment.

Molecular Signatures Altered with HPGCD Treatment Are Different from Those with HPBCD Treatment

To further characterize the HPBCD and HPGCD effects on NPC-derived HLCs, we analyzed gene expression profiles from the microarray experiments. The patterns of global gene expression were similar between untreated HLCs and cells treated with HPBCD (Fig. 5D; Supporting Information Fig. S7B), but different with HPGCD treatment (Fig. 5E; Supporting Information Fig. S7C). Interestingly however, there were differences in specific gene expression patterns between HPGCD-treated and HPBCD-treated HLCs, suggesting that HPGCD and HPBCD have different effects on iPSC-derived HLCs at the molecular level (Fig. 5F; Supporting Information Fig. S7D). Further GSEA to explore the functional significance of changes in gene expression with HPGCD and HPBCD treatments revealed the specific molecular signatures in the commonly downregulated genes in NPC-derived HLCs (Fig. 5A). The one molecular signatures significantly altered by the HPBCD treatment relate functionally to immunity ($p < .05$; Fig. 5G). HPGCD treatment significantly changed gene expression patterns related to three molecular signatures ($p < .05$; Fig. 5G). The molecular signatures related to chemical stimulus response and cell-cell signaling were significantly identified in the HPGCD-treated cells, but not in the HPBCD-treated cells. In the top-10 signatures, some molecular signatures such as lipid metabolism were affected by both cyclodextrin treatments (Fig. 5G). The cluster analysis revealed that HPGCD treatment shifted HPBCD-altered signature with $p < .05$ closer to the normal pattern than HPBCD (Supporting Information Fig. S7E). However, HPGCD-altered signature with $p < .05$, as shown in Figure 5G, did not show this tendency (Supporting Information Fig. S7E). We also analyzed the top-10 signatures together. Interestingly, while HPGCD treatment shifted HPGCD-altered signatures closer to the normal pattern than HPBCD, HPBCD treatment shifted the HPBCD-altered signatures closer to the normal pattern than HPGCD (Supporting Information Fig. S7F). We attempted to enrich the molecular signatures identified in the commonly upregulated genes of HLCs derived from NPC-iPSC lines, but found no effect with either HPBCD or HPGCD treatment. The fact that some molecular signatures were common and others specifically and significantly changed by HPGCD treatment only suggests that the molecular mechanisms underlying the cholesterol reduction are different between HPBCD and HPGCD treatments, although they share some common mechanisms. The results of DNA arrays were confirmed by quantitative RT-PCR of the genes that were randomly selected from the heatmap (Supporting Information Figs. S8–S11).

HPGCD Treatment Can Improve NPC-Model Mice

Herein we identified a novel effect of HPGCD on the reduction of cholesterol accumulation in NPC-derived HLCs. Next, we asked whether HPGCD treatment could be similarly effective in NPC model mice bearing a spontaneous mutation of the *Npc1* gene that causes a defect in lysosome to ER trafficking of cholesterol. These mice also exhibit a similar phenotype to the human disease including cholesterol accumulation in the liver and brain. The model mice show liver injury and neural functional impairment and die before 12 weeks old without proper treatment [32].

We treated 4-week-old NPC mice with HPGCD once a week until 8.5 weeks of age (Fig. 6A) by subcutaneous injection (five injections in total). Following treatment, aspartate aminotransferase and alanine aminotransferase, serum markers for liver injury, were markedly and significantly reduced (Fig. 6B), and histological analysis revealed a marked morphological improvement in the livers of mice treated with HPGCD (Fig. 6C). Vacuolization and lipid-laden macrophages observed in the livers of saline-treated NPC mice were almost absent in the treated mice (Fig. 6C; Supporting Information Fig. S12A). Consistently, the free cholesterol accumulation was significantly decreased in the livers of the HPGCD-treated mice, compared to those of saline-treated mice (Fig. 6D). Interestingly, Purkinje cells of HPGCD-treated mice still partially remained in the cerebellar vermis, comparing to the saline-treated NPC mice (Fig. 6E; Supporting Information Fig. S12A), suggesting that HPGCD injection affects both liver and cerebellar defects in the NPC model mice.

Cellular markers of autophagy such as LC3-II and insoluble p62 were upregulated in the livers and brains of saline-treated NPC mice, and then significantly reduced with the HPGCD treatment (Fig. 6F), indicating that HPGCD could also recover autophagy function in the liver and brain of NPC model mice.

Survival analysis shows that the HPGCD treatment could significantly prolong the NPC mouse survival by 10–14 days (Fig. 6G). To clarify the cause of death in the treated mice, we carefully and extensively examined the pathology of the organs such as heart, lung, liver, kidney, and cerebellum in the dead mice. Many vacuoles were observed in the liver and kidney of the saline-treated mice, suggesting that free cholesterol and glycolipids are accumulated in them (Fig. 6H;

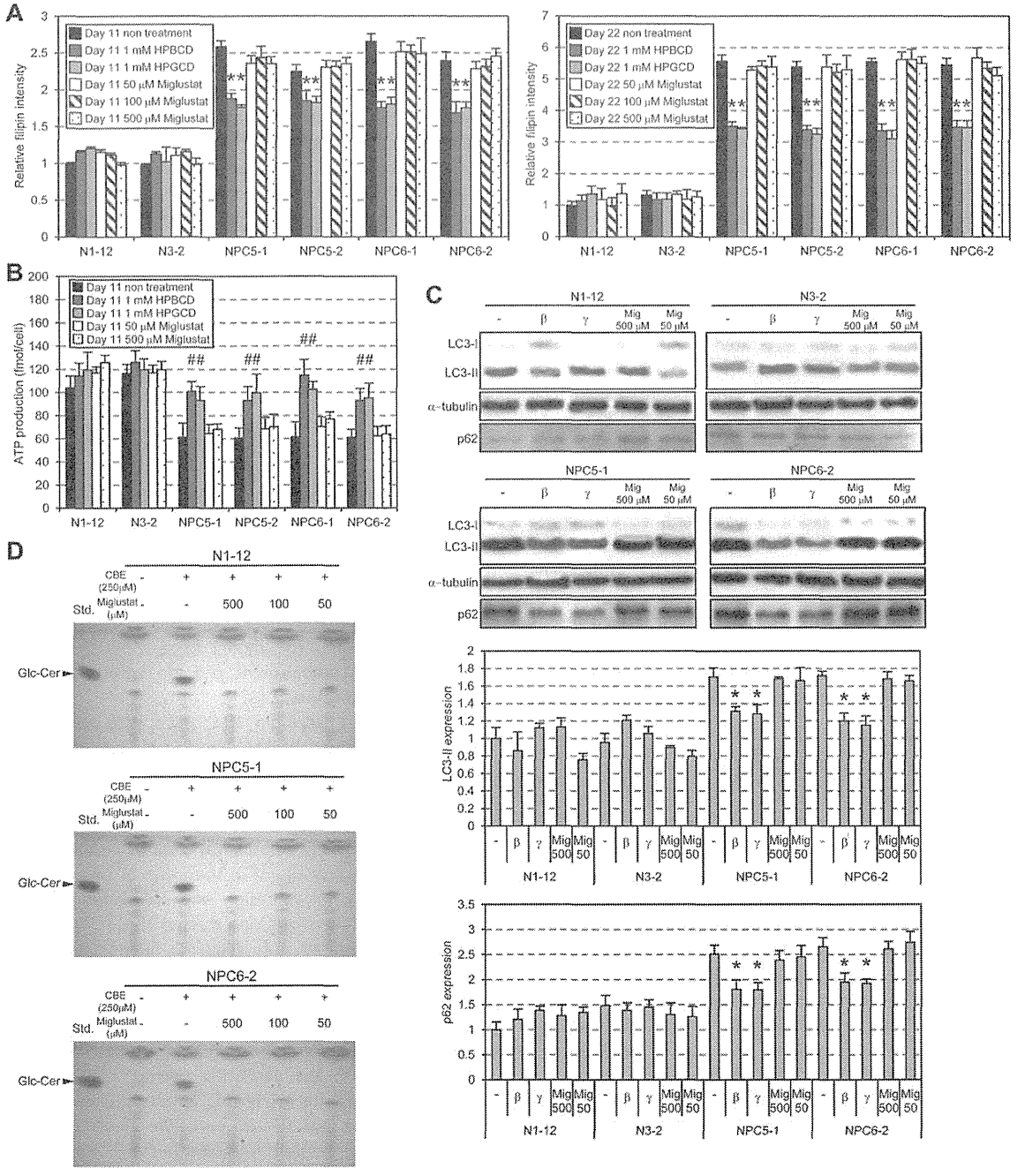

Figure 4. Action mechanism of 2-hydroxypropyl-cyclodextrin (HPCD) is different from Miglustat. **(A):** Effect of Miglustat on the free cholesterol accumulation in the NPC-derived cells. Neural progenitors (left graph) and hepatocyte-like cells (right graph) were cultured with the various concentration of Miglustat and 1 mM of the indicated hydroxypropyl-cyclodextrin for 4 days, filipin stained, and analyzed with an IN Cell Analyzer. Miglustat did not reduce the cholesterol accumulation. Data are means ± SD of three independent experiments. *, $p < .01$, nontreatment versus treatment of each NPC-derived cells, Student's t test. **(B):** HPBCD and HPGCD but not Miglustat treatments restored ATP levels of NPC-derived neural progenitors. The levels were significantly recovered by treatments with HPBCD and HPGCD. Data are means ± SD of three independent experiments. #, $p < .05$, nontreatment versus treatment, Student's t test. **(C):** HPCD but not Miglustat treatments restored the abnormal autophagy in NPC-derived neural progenitors. The expression levels of LC3 and p62 were decreased by treatments with HPBCD and HPGCD. In contrast, Miglustat did not affect the expression levels of LC3 and p62. β: Treatment with 1 mM HPBCD for 4 days, γ: 1 mM HPGCD treatment for 4 days, Mig: Treatment with the indicated concentration of Miglustat for 4 days. The expression level was normalized to α-tubulin expression in each iPSC line. **(D):** Miglustat can inhibit the synthesis of glycosylceramide in NPC-derived neural progenitors. The glycosylceramide expression disappeared with Miglustat treatment, suggesting that Miglustat inhibit the synthesis of glycosylceramide by blocking the activity of glycosylceramide synthase. Abbreviations: CBE, conduritol B epoxide, inhibitor of β-glucocerebrosidase; Glc-Cer, glycosylceramide; HPBCD, 2-hydroxypropyl-β-cyclodextrin; HPGCD, 2-hydroxypropyl-γ-cyclodextrin; NPC, Niemann-Pick disease type C; Std, glycosylceramide as a standard.

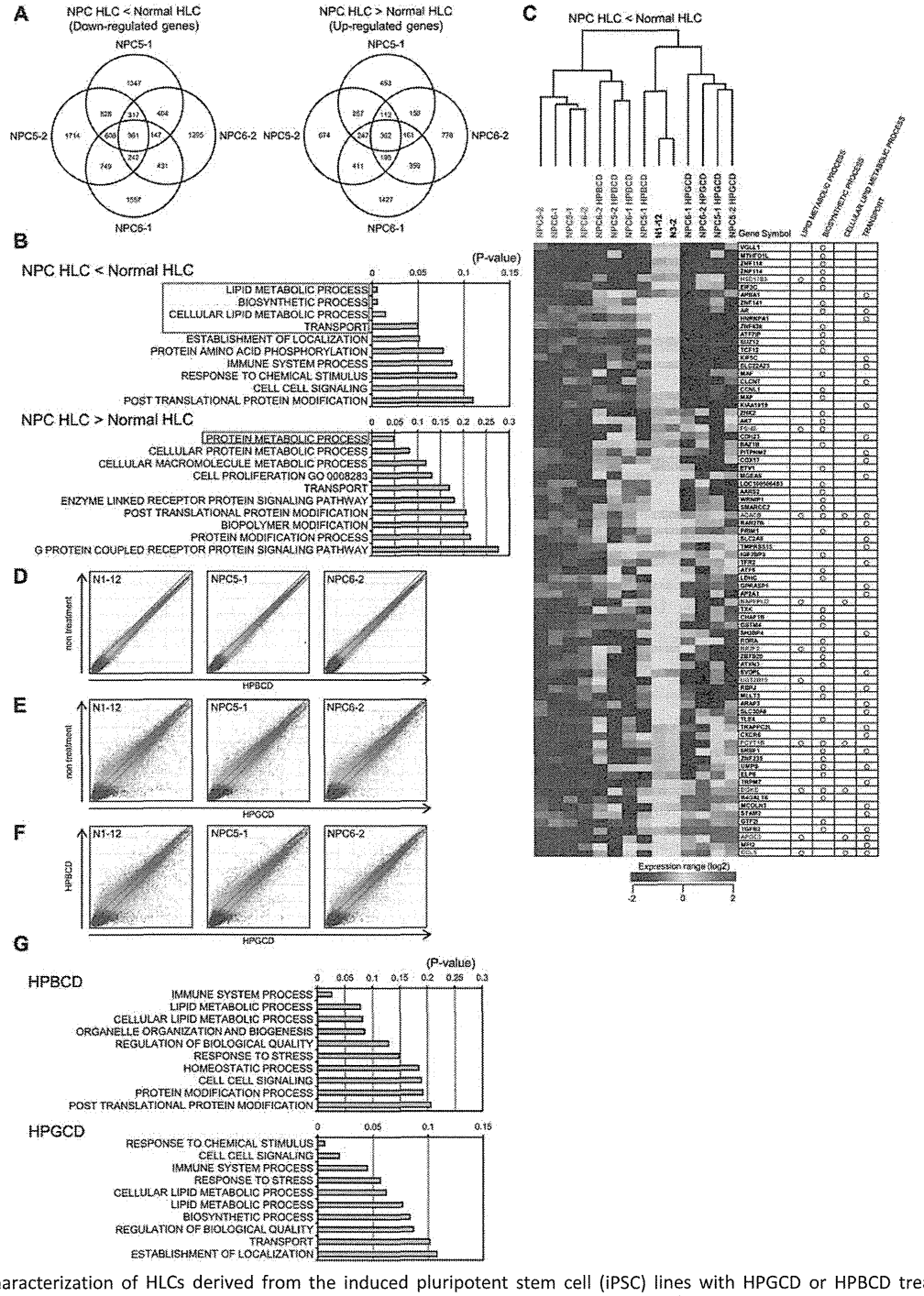

Figure 5. Characterization of HLCs derived from the induced pluripotent stem cell (iPSC) lines with HPGCD or HPBCD treatments. **(A):** Venn diagram for the genes that were downregulated or upregulated by 1.5-fold or more between healthy donor- and NPC-derived HLCs. Comparing downregulated or upregulated gene profiles between healthy donor- and NPC-derived HLCs, the gene expressions of 361 datasets were commonly downregulated (left panel) and those of 362 datasets were upregulated (right panel). **(B):** Molecular signatures were altered in NPC-derived HLCs. Gene set enrichment analysis (GSEA) enriched the biological processes of gene ontology, which are significantly altered in NPC-derived HLCs. The molecular signatures in the red squares were significantly ($p < .05$) changed in NPC-derived HLCs, compared to healthy donor-derived HLCs. Upper graph: downregulated signatures in NPC, lower graph: upregulated signatures in NPC. **(C):** Hierarchical clustering of genes significantly downregulated in NPC. The datasets of the genes included in the molecular signatures as shown in the red square of Figure 5B were clustered according to Euclidean distance metrics. The datasets of NPC-derived HLCs with HPGCD treatment (blue) were close to those of normal HLCs (black). In contrast, the datasets of NPC-derived HLCs (pink) and three out of four with HPBCD treatments (green) were classified into the separate branch from those of normal HLCs. The genes selected are classified into the four signatures: lipid metabolic process, biosynthetic process, cellular lipid metabolic process, and transport (right panel). Red gene names indicate those genes included in the Lipid metabolic process. **(D–F):** Global gene-expression patterns of the HLCs following HPBCD and HPGCD treatments. Scatter-plot representations of the global gene-expression patterns for HLCs in the presence and absence of HPBCD (D) or HPGCD (E) were compared. In addition, scatter-plot representations of the global gene-expression patterns for the HLCs with HPGCD treatment were compared to those with HPBCD treatment (F). The pattern of global gene expression for HLCs with HPGCD treatment is different from that with no treatment or HPBCD treatment. N1–12 and N3-2: HLCs derived from normal iPSC lines; NPC5-1, NPC5-2, NPC6-1, and NPC6-2: HLCs derived from NPC-iPSC lines. **(G):** Some molecular signatures specifically altered with HPGCD treatment differed from those altered with HPBCD treatment. In the commonly downregulated genes in NPC-derived HLCs (Fig. 5A), GSEA enriched the biological processes containing the genes that were significantly changed with HPBCD (upper) or HPGCD (lower) treatments. The molecular signatures including response to chemical stimulus and cell signaling were specifically and significantly altered with HPGCD treatment ($p < .05$). Abbreviations: HLC, hepatocyte-like cell; HPBCD, 2-hydroxypropyl-β-cyclodextrin; HPGCD, 2-hydroxypropyl-γ-cyclodextrin; NPC, Niemann-Pick disease type C.

Supporting Information Fig. S12B). In contrast, the organs of the HPGCD-treated mice look normal with no vacuoles. However, the defect of Purkinje cells in the cerebellum was exacerbated and was not at all improved even with the HPGCD treatment (Fig. 6I; Supporting Information Fig. S12B). Consistently, the cholesterol accumulation was not reduced in the brain of HPGCD-treated mice (Supporting Information Fig. S12C). Based on these results, we concluded that HPGCD-treated mice died due to the neurological disturbance.

Finally, we examined the toxic effects of HPBCD and HPGCD in vitro and in vivo. HPGCD was much less toxic than HPBCD in both iPSC-derived HLCs and normal mice (Fig. 7A, 7B). Indeed, high-dose HPBCD treatment decreased cell viability and mouse survival rate, whereas similar doses of HPGCD had no effect on cell viability and mouse survival rate. Interestingly, the NPC-derived HLCs showed less toxicity to HPBCD treatment than normal HLCs (Fig. 7A). These data suggest that HPGCD is a safer candidate than HPBCD for NPC therapy in the future. Taken together, our results indicate that HPGCD treatment can improve the abnormalities in NPC model mice and that HPGCD is a potential drug candidate for NPC treatment.

Discussion

We established iPSC lines from two patients with NPC and demonstrated that these lines provide an appropriate cellular model of the disease. Using the model, we found a new drug candidate, HPGCD, for NPC therapy.

Our finding that free cholesterol accumulated in HLCs and neural progenitors derived from NPC-iPSC lines was consistent with the cholesterol accumulation observed in the livers and brains of NPC patients [18]. Biochemical analysis revealed low ATP production and abnormal autophagy in the NPC-derived HLCs and neural progenitors compared with the normal controls. These low ATP levels are consistent with the abnormally low levels of ATP observed in the brain, muscle, and liver of 9-week-old *Npc1*-null mice [33], and although we found no differences in the mitochondrial membrane potentials, the low ATP levels also suggested that reduced mitochondrial activity in HLCs and neural progenitors is an early event of NPC. Reduction in mitochondrial activity occurs in the early phases of apoptosis, as detected in the liver tissue of adult *Npc1* null mice (more than 7 weeks old), but not young *Npc1* null mice (less than 7 weeks old) [34]. Here, we found no evidence of enhanced apoptosis in NPC-HLCs newly generated from NPC-derived iPSC lines, suggesting that cellular apoptosis is not a feature of the early disease phase, despite the cholesterol accumulation.

Both HLCs and neural progenitors derived from NPC-iPSCs showed elevated protein levels of LC3-II and insoluble p62, as well as abnormal p62 aggregation, compared to those derived from normal controls. LC3-II is a robust marker for autophagy induction, and impairment of autophagic flux is associated with accumulation of insoluble p62, which forms abnormal aggregates [26, 27]. Therefore, our results suggest that the *NPC1* mutation in the iPSC-derived HLCs and neural progenitors caused both induction of autophagy and impairment of autophagic flux. Abnormal autophagic events are widely observed in lysosomal storage diseases [25], and a marked accumulation of autophagosomes is observed in the liver tissues of *Npc1*-null mice and fibroblasts of NPC patients [35, 36]. Taken together, our results therefore suggested that both reduced ATP levels and enhanced autophagy induction are early pathogenic events of NPC.

In this study, GSEA revealed that lipid and protein metabolism were significantly impaired in NPC-derived HLCs. Cholesterol and glycosphingolipids are key molecules in the pathogenesis of NPC, and previous studies implicated molecular pathways related to lipid metabolism in the liver and brain abnormalities observed in NPC mice [34, 37]. However, because these previous results were obtained from the tissues and organs of NPC mice, it could not be determined whether the pathways were directly affected by the NPC mutation or were secondary effects to tissue destruction processes such as inflammation. Moreover, it is still unclear whether cyclodextrin treatments can restore the abnormal molecular pathways observed in NPC cells. In this study, HPBCD treatment reduced cholesterol accumulation in NPC-iPSC-derived HLCs and neural progenitors. This result confirms and extends the previous findings that HPBCD treatment effectively reduces cholesterol accumulation in *Npc1*-null mice and NPC-derived fibroblasts [38–40].

We newly found that HPGCD treatment also effectively reduced cholesterol accumulation in NPC-derived HLCs and neural progenitors, but that HPACD had no effect. In addition, both HPBCD and HPGCD restored ATP levels and abnormal autophagy in NPC-derived HLCs and neural progenitors, and HPGCD treatment dramatically improved liver injury and abnormal autophagy in NPC mice, as well as prolonging survival. Moreover, cerebellar Purkinje cell defects in the model mice were partially improved with HPGCD treatment. Previous study demonstrated that HPBCD could not enter the central nervous system (CNS) through the blood brain barrier (BBB) in normal and NPC model mice. However, a volume of distribution available to HPBCD exceeded the accepted values for plasma and vascular volume of the brain, indicating a considerable cell surface binding of HPBCD to the endothelium of the cerebral vasculature. This may provide a favorable influence to normalize the biochemical and morphological abnormality of CNS in NPC model mice [41]. In a similar manner to HPBCD, the molecular weight of HPGCD (1,668 Da) prevents it from transiting the BBB. The mechanism underlying the effect on the cerebellar Purkinje cell is still unclear and further studies are needed to elucidate it.

Although the HPGCD treatment with the subcutaneous injection prolonged the mice survivals, the treated mice finally died due to the neurological disturbance. Histological analyses could not find any marked abnormality in the lung, heart, kidney, and liver of the HPGCD-treated mice. These results suggest that HPGCD treatment is effective on the major organs except for the CNS. The intrathecal injection of HPGCD should be considered to treat the neurological disturbance of NPC mice.

HPACD, HPBCD, and HPGCD consist of six, seven, and eight D-glucopyranose units, respectively, linked to 2-hydroxypropyl groups by α-1,4 glycosidic bonds to form a macrocycle [42]. This structure provides the cyclodextrins with a hydrophilic outer surface and a somewhat hydrophobic central cavity. The ability of each hydroxypropyl-cyclodextrin to form inclusion complexes with specific guest molecules

depends upon the cavity size. For instance, the acyl chain of phospholipids fits tightly into the small hydrophobic cavity of HPACD, whereas the side chain of cholesterol is preferentially included in the larger inner space of the HPBCD and HPGCD cavities [43]. Thus, our observation that HPBCD and HPGCD, but not HPACD, were effective in reducing cholesterol

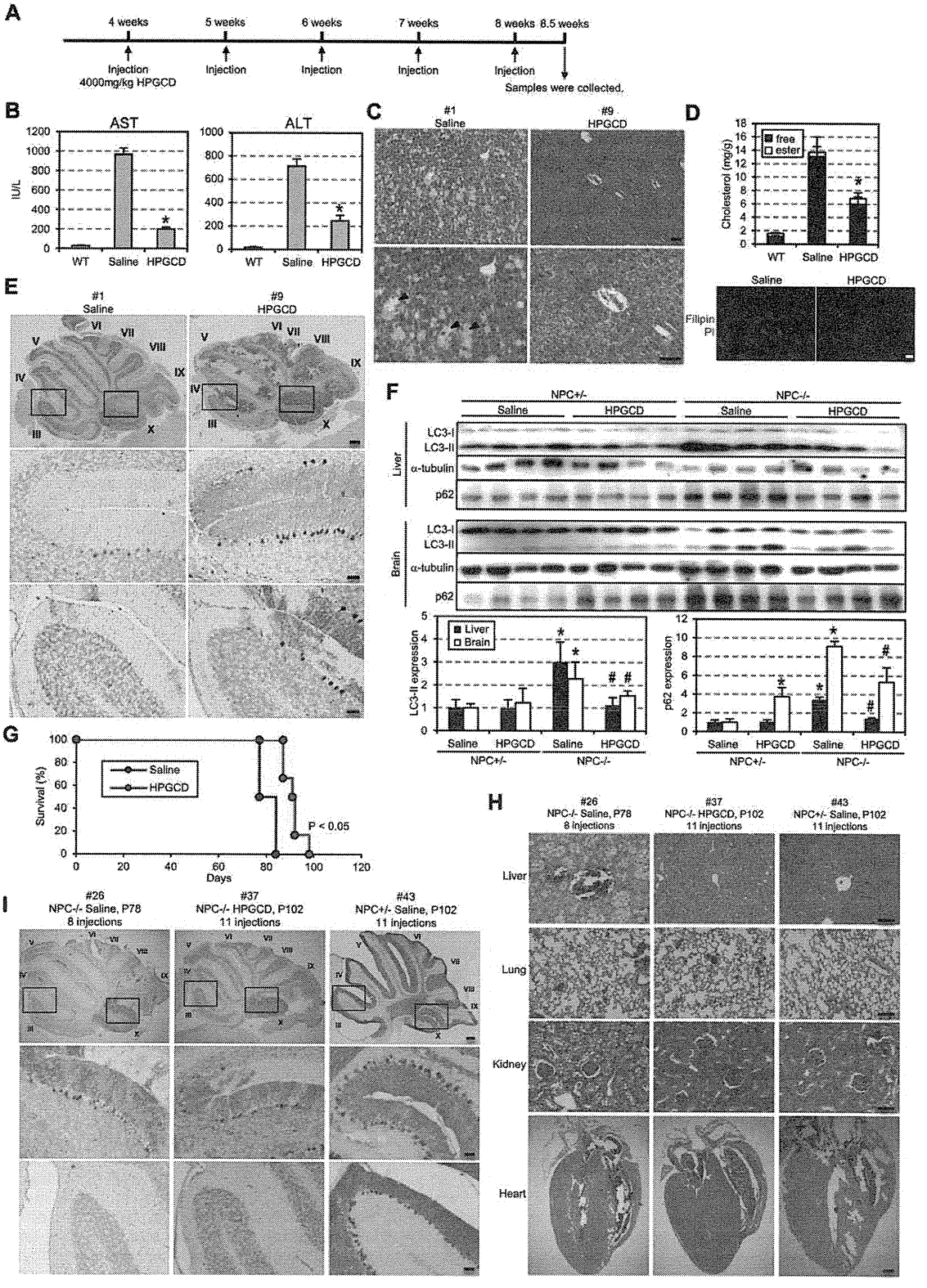

Figure 6.

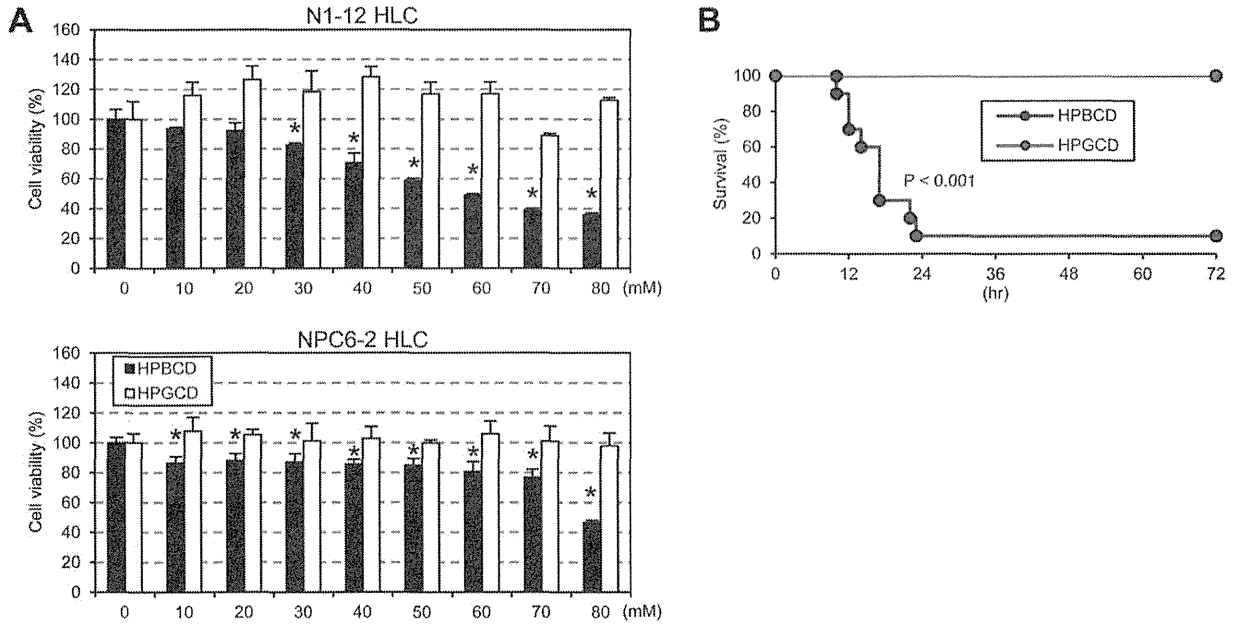

Figure 7. Toxicities of HPGCD are smaller than those of HPBCD. **(A):** In vitro cell toxicity testing of HLCs treated with HPBCD and HPGCD. Healthy donor- and NPC-derived iPSCs were induced into HLCs and the cell survival rates were determined with various HPBCD and HPGCD concentrations. Data are means ± SD of three independent experiments. *, $p < .01$, nontreatment versus treatment, Student's *t* test. **(B):** Acute toxicity test of normal mice given HPBCD and HPGCD injections. 14.4 mM HPBCD and HPGCD were injected into the subcutaneous tissues of 8-week-old mice ($n = 10$ each), and then survival rates were calculated. Almost all mice injected with HPBCD died up to 72 hours after the injection. In contrast, no mice died with the HPGCD injection. Abbreviations: HLC, hepatocyte-like cell; HPBCD, 2-hydroxypropyl-β-cyclodextrin; HPGCD, 2-hydroxypropyl-γ-cyclodextrin; NPC, Niemann-Pick disease type C.

accumulation in NPC-HLCs is consistent with these structural differences. Although both HPGCD and HPBCD treatments can reduce the cholesterol accumulation in HLCs and neural progenitors, some gene signatures altered with HPGCD treatment are shown to be different from those with HPBCD treatment. Both HPGCD and HPBCD treatments improved the abnormal molecular signatures in NPC-derived HLCs. In our system, Miglustat could not improve the cholesterol accumulation,

Figure 6. NPC model mice treated with HPGCD. **(A):** Injection schedule of HPGCD into NPC model mice. HPGCD was subcutaneously injected into NPC model mice once a week from 4 weeks to 8 weeks of age, and the mice treated with HPGCD were analyzed at 8.5 weeks old. Experiments were done twice (first; $n = 6$ each and second; $n = 4$ each). **(B):** Levels of AST and ALT in the serum of NPC model mice were markedly and significantly reduced with HPGCD treatment, compared to saline-treated mice. Data are means ± SD of two independent experiments (experiment 1: $n = 6$ each, experiment 2: $n = 4$ each). WT: wild type mice ($n = 4$), experiment 1 only. *, $p < .01$, saline versus HPGCD treatments, Student's *t* test. **(C):** Representative histological sections of liver from the NPC model mice with saline and HPGCD treatments. Liver histology was greatly improved with HPGCD treatment. Arrow heads indicate lipid-laden macrophages. Upper images: low magnification (×200), lower images: high magnification (×400). Scale bars = 50 μm. **(D):** Levels of cholesterol in the mice treated with HPGCD. The level of free cholesterol was markedly and significantly reduced in the livers of mice treated with HPGCD, compared to saline-treated controls (upper graph). Consistently, positive filipin staining was weaker in the HPGCD-treated mice than in saline-treated controls (lower images, representative data). Data are means ± SD of two independent experiments (Experiment 1: $n = 6$ each, Experiment 2: $n = 4$ each). *, $p < .01$, saline versus HPGCD treatments, Student's *t* test. Scale bars = 50 μm. **(E):** Representative histological sections of cerebellar vermis from the NPC model mice with HPGCD treatment. The Purkinje cells partially remained in HPGCD-treated mice (right images), comparing to saline-treated mice (left images). The sections were stained for calbindin immunoreactivity. The areas surrounded by the squares (upper images) are shown in the middle and lower images. Upper images: low magnification (×40), scale bars = 200 μm. Middle and lower images: high magnification (×200). Scale bars = 50 μm. **(F):** Abnormal autophagy was restored in NPC model mice with HPGCD treatment. The expression levels of LC3 and insoluble p62 in mice liver and brain were recovered to normal levels by treatments with HPGCD. The expression level was normalized to α-tubulin expression in each sample. The Western blot data (upper images) are summarized in the lower graphs. Data are means ± SD of four mice. #, $p < .05$; *, $p < .01$, saline versus HPGCD treatments, Student's *t* test. **(G):** Survival curve for mice with HPGCD treatment. HPGCD treatment prolonged the survival of NPC model mice. A total of 12 mice were injected with saline or HPGCD ($n = 6$ each) once a week from 4 weeks old. **(H):** Representative histological analyses of the major organs in the dead mice. A number of abnormal vacuoles were observed in the liver and kidney of saline-treated mice. In contrast, almost all organ histology did not exhibit marked abnormality in HPGCD-treated mice. HE staining. Scale bars: liver = 50 μm; lung = 100 μm; kidney = 50 μm; heart = 500 μm. P78, P102, P102: ages of dying or analyzing. **(I):** Representative histological sections of cerebellar vermis from the dead mice. Comparing to the heterozygous mouse (right images), the large defect of Purkinje cells was observed in both mice except for region X (left and center images). The sections were stained for calbindin immunoreactivity. Same mice as shown in Figure 6H. The areas surrounded by the squares (upper images) are shown in the middle and lower images. Upper images: low magnification (×40), scale bars = 200 μm. Middle and lower images: high magnification (×200). Scale bars = 50 μm. Abbreviations: ALT, alanine aminotransferase; AST, aspartate aminotransferase; HPGCD, 2-hydroxypropyl-γ-cyclodextrin; NPC, Niemann-Pick disease type C.

ATP level, and abnormal autophagy in HLCs and neural progenitors. These results suggest that HPGCD could remove the accumulation of cholesterol from NPC-derived HLCs by a different mechanism from that used by HPBCD and Miglustat, in that HPGCD and HPBCD treatments significantly altered different molecular signatures. The cluster analyses of genes in the abnormal signature revealed that HPGCD treatment could rescue the abnormal expression patterns of genes to a status closer to that of normal HLCs than HPBCD treatment. The result suggests that HPGCD treatment can correct the abnormal patterns of gene expression induced by NPC more effectively than HPBCD treatment.

We also demonstrated that the intermittent injections of HPGCD could partially rescue the liver injury typical of NPC model mice and prolong their survival. Consistently, the abnormal liver histology was also improved by HPGCD treatment, with an efficiency similar to that previously demonstrated for HPBCD treatment [44, 45]. However, we showed HPGCD to be safer than HPBCD in terms of acute toxicities in vitro and in vivo, and indeed, one of the most important requirements for drug candidates is no or acceptably low levels of intrinsic cytotoxicity. Additionally, our study revealed that high-dose treatments with HPGCD, but not HPBCD, had no effect on cell viability and mouse survival. Future in vitro lysis of isolated erythrocytes might provide a simple and reliable measure of cyclodextrin toxicity because the interaction between these drug molecules and the plasma membrane is the initial step any such cell damage. The hemolytic activity of the hydroxypropyl-cyclodextrins is reportedly in the order HPBCD > HPACD > HPGCD [43], and previous studies indicated that γ-cyclodextrin is safer than α- or β-cyclodextrin for acute intravenous administration in rats, in which the intravenous doses that are lethal to 50% of population (LD50 values) are 1,000, 788, and >3,750 mg/kg for α-, β-, and γ-cyclodextrins, respectively [46, 47]. These study findings are supported by all these previous results. In addition, HPGCD-based pharmaceutical products, such as eye drops, intravenous solutions, and intramuscular solutions, have been used clinically [48]. Therefore, although the safety data for HPGCD provided by this study are limited, our results indicated that HPGCD is a promising candidate for the treatment of NPC. Based on the results from the DNA array and safety examinations, HPGCD outperforms HPBCD as a potential treatment for NPC.

Disease-derived iPSCs generated using the SeV vector are highly suitable for studying disease because the vector never integrates into the host genome, and herein, we have thus established a novel cellular model of NPC using transgene-free iPSCs, and have revealed new drug candidate for the future therapy. Biosamples collected from NPC patients are essential for studying the mechanisms of diseases and developing new therapies, but tissue collection is difficult because of the limited numbers of patients and the inaccessibility of target cells such as liver and neural cells. The transgene-free iPSC lines developed in this study will become indispensable tools for facilitating the development of new and much-awaited therapeutic agents for treating NPC patients.

Conclusions

In summary, the disease model of NPC-derived iPSC lines is useful for studying the pathological events and HPGCD is a potential candidate as a future drug for NPC.

Acknowledgments

We would like to thank Toyoko Tsuru, Yumi Soejima, and Kousaku Ohno for providing NPC model mice and technical support. This study was supported in part by grants from the Ministry of Health, Labor, and Welfare of Japan, Precursory Research for Embryonic Science and Technology (PRESTO), Core Research for Evolutional Science and Technology (CREST), and Japan Science and Technology Agency (JST). N.F. is currently affiliated with the Department of Ophthalmology, Keio University School of Medicine, 35 Shinano-machi, Shinjuku-ku, Tokyo 160–8582, Japan. H.F. is currently affiliated with the Department of Neurology, Kochi Medical School, Okatoyo-machi, Nangoku city, Kochi 783-8505, Japan.

Author Contributions

T.E.: designed all experiments, wrote and prepared the manuscript, and edited the manuscript; T.I.: designed the in vivo experiment involving HPGCD injections, provided the chemicals, and edited the manuscript; Y.I., M.S., M.H., K.Y., and N.N.: performed the experiments and analyzed data and edited the manuscript; N.F.: designed, produced, and provided the Sendai virus vectors and edited the manuscript; H.F., H.I., M.M., K.N., and F.E.: provided the patient samples and data and edited the manuscript.

Disclosure of Potential Conflicts of Interest

The authors indicate no potential conflicts of interest.

References

1 Takahashi K, Tanabe K, Ohnuki M et al. Induction of pluripotent stem cells from adult human fibroblasts by defined factors. Cell 2007;131:861–872.

2 Yu J, Vodyanik MA, Smuga-Otto K et al. Induced pluripotent stem cell lines derived from human somatic cells. Science 2007;318:1917–1920.

3 Avilion AA, Nicolis SK, Pevny LH et al. Multipotent cell lineages in early mouse development depend on SOX2 function. Genes Dev 2003;17:126–140.

4 Takahashi K, Yamanaka S. Induction of pluripotent stem cells from mouse embryonic and adult fibroblast cultures by defined factors. Cell 2006;126:663–676.

5 Nichols J, Zevnik B, Anastassiadis K et al. Formation of pluripotent stem cells in the mammalian embryo depends on the POU transcription factor Oct4. Cell 1998;95:379–391.

6 Seki T, Yuasa S, Oda M et al. Generation of induced pluripotent stem cells from human terminally differentiated circulating T cells. Cell Stem Cell 2010;7:11–14.

7 Ban H, Nishishita N, Fusaki N et al. Efficient generation of transgene-free human induced pluripotent stem cells (iPSCs) by temperature-sensitive Sendai virus vectors. Proc Natl Acad Sci USA 2011;108:14234–14239.

8 Ebert AD, Yu J, Rose FF, Jr. et al. Induced pluripotent stem cells from a spinal muscular atrophy patient. Nature 2009;457:277–280.

9 Marchetto MC, Carromeu C, Acab A et al. A model for neural development and treatment of Rett syndrome using human induced pluripotent stem cells. Cell 2010;143:527–539.

10 Liu GH, Suzuki K, Qu J et al. Targeted gene correction of laminopathy-associated LMNA mutations in patient-specific iPSCs. Cell Stem Cell 2011;8:688–694.
11 Yusa K, Rashid ST, Strick-Marchand H et al. Targeted gene correction of alpha1-antitrypsin deficiency in induced pluripotent stem cells. Nature 2011;478:391–394.
12 Tanaka A, Woltjen K, Miyake K et al. Efficient and reproducible myogenic differentiation from human iPS cells: Prospects for modeling Miyoshi Myopathy in vitro. PLoS One 2013;8:e61540.
13 Tulpule A, Kelley JM, Lensch MW et al. Pluripotent stem cell models of Shwachman-Diamond syndrome reveal a common mechanism for pancreatic and hematopoietic dysfunction. Cell Stem Cell 2013;12:727–736.
14 Hamasaki M, Hashizume Y, Yamada Y et al. Pathogenic mutation of ALK2 inhibits induced pluripotent stem cell reprogramming and maintenance: Mechanisms of reprogramming and strategy for drug identification. Stem Cells 2012;30:2437–2449.
15 Kondo T, Asai M, Tsukita K et al. Modeling Alzheimer's disease with iPSCs reveals stress phenotypes associated with intracellular Abeta and differential drug responsiveness. Cell Stem Cell 2013;12:487–496.
16 Carstea ED, Morris JA, Coleman KG et al. Niemann-Pick C1 disease gene: Homology to mediators of cholesterol homeostasis. Science 1997;277:228–231.
17 Naureckiene S, Sleat DE, Lackland H et al. Identification of HE1 as the second gene of Niemann-Pick C disease. Science 2000;290:2298–2301.
18 Vanier MT. Niemann-Pick disease type C. Orphanet J Rare Dis 2010;5:16.
19 Heron B, Valayannopoulos V, Baruteau J et al. Miglustat therapy in the French cohort of paediatric patients with Niemann-Pick disease type C. Orphanet J Rare Dis 2012;7:36.
20 Fusaki N, Ban H, Nishiyama A et al. Efficient induction of transgene-free human pluripotent stem cells using a vector based on Sendai virus, an RNA virus that does not integrate into the host genome. Proc Jpn Acad Ser B Phys Biol Sci 2009;85:348–362.
21 Tada S, Era T, Furusawa C et al. Characterization of mesendoderm: A diverging point of the definitive endoderm and mesoderm in embryonic stem cell differentiation culture. Development 2005;132:4363–4374.
22 Yasunaga M, Tada S, Torikai-Nishikawa S et al. Induction and monitoring of definitive and visceral endoderm differentiation of mouse ES cells. Nat Biotechnol 2005;23:1542–1550.
23 Macho A, Decaudin D, Castedo M et al. Chloromethyl-X-Rosamine is an aldehyde-fixable potential-sensitive fluorochrome for the detection of early apoptosis. Cytometry 1996;25:333–340.
24 Smiley ST, ReersM, Mottola-Hartshorn C et al. Intracellular heterogeneity in mitochondrial membrane potentials revealed by a J-aggregate-forming lipophilic cation JC-1. Proc Natl Acad Sci USA 1991;88:3671–3675.
25 Lieberman AP, Puertollano R, Raben N et al. Autophagy in lysosomal storage disorders. Autophagy 2012;8:719–730.
26 Kabeya Y, Mizushima N, Ueno T et al. LC3, a mammalian homologue of yeast Apg8p, is localized in autophagosome membranes after processing. EMBO J 2000;19:5720–5728.
27 Komatsu M, Waguri S, Koike M et al. Homeostatic levels of p62 control cytoplasmic inclusion body formation in autophagy-deficient mice. Cell 2007;131:1149–1163.
28 Camargo F, Erickson RP, Garver WS et al. Cyclodextrins in the treatment of a mouse model of Niemann-Pick C disease. Life Sci 2001;70:131–142.
29 Group N-CGW, Wraith JE, Baumgartner MR et al. Recommendations on the diagnosis and management of Niemann-Pick disease type C. Mol Genet Metab 2009;98:152–165.
30 Patterson MC, Vecchio D, Prady H et al. Miglustat for treatment of Niemann-Pick C disease: A randomised controlled study. Lancet Neurol 2007;6:765–772.
31 Platt FM, Neises GR, Dwek RA et al. N-Butyldeoxynojirimycin is a novel inhibitor of glycolipid biosynthesis. J Biol Chem 1994;269:8362–8365.
32 Loftus SK, Morris JA, Carstea ED et al. Murine model of Niemann-Pick C disease: Mutation in a cholesterol homeostasis gene. Science 1997;277:232–235.
33 Yu W, Gong JS, Ko M et al. Altered cholesterol metabolism in Niemann-Pick type C1 mouse brains affects mitochondrial function. J Biol Chem 2005;280:11731–11739.
34 Cluzeau CV, Watkins-Chow DE, Fu R et al. Microarray expression analysis and identification of serum biomarkers for Niemann-Pick disease, type C1. Hum Mol Genet 2012;21:3632–3646.
35 Pacheco CD, Elrick MJ, Lieberman AP. Tau deletion exacerbates the phenotype of Niemann-Pick type C mice and implicates autophagy in pathogenesis. Hum Mol Genet 2009;18:956–965.
36 Pacheco CD, Kunkel R, Lieberman AP. Autophagy in Niemann-Pick C disease is dependent upon Beclin-1 and responsive to lipid trafficking defects. Hum Mol Genet 2007;16:1495–1503.
37 Liao G, Wen Z, Irizarry K et al. Abnormal gene expression in cerebellum of Npc1-/- mice during postnatal development. Brain Res 2010;1325:128–140.
38 Davidson CD, Ali NF, Micsenyi MC et al. Chronic cyclodextrin treatment of murine Niemann-Pick C disease ameliorates neuronal cholesterol and glycosphingolipid storage and disease progression. PLoS One 2009;4:e6951.
39 Liu B, Li H, Repa JJ et al. Genetic variations and treatments that affect the lifespan of the NPC1 mouse. J Lipid Res 2008;49:663–669.
40 Rosenbaum AI, Zhang G, Warren JD et al. Endocytosis of beta-cyclodextrins is responsible for cholesterol reduction in Niemann-Pick type C mutant cells. Proc Natl Acad Sci USA 2010;107:5477–5482.
41 Pontikis CC, Davidson CD, Walkley SU et al. Cyclodextrin alleviates neuronal storage of cholesterol in Niemann-Pick C disease without evidence of detectable blood-brain barrier permeability. J Inher Metab Dis 2013;36:491–498.
42 Uekama K, Hirayama F, Irie T. Cyclodextrin drug carrier systems. Chem Rev 1998;98:2045–2076.
43 Irie T, Uekama K. Pharmaceutical applications of cyclodextrins. III. Toxicological issues and safety evaluation. J Pharm Sci 1997;86:147–162.
44 Ramirez CM, Liu B, Taylor AM et al. Weekly cyclodextrin administration normalizes cholesterol metabolism in nearly every organ of the Niemann-Pick type C1 mouse and markedly prolongs life. Pediatr Res 2010;68:309–315.
45 Liu B, Turley SD, Burns DK et al. Reversal of defective lysosomal transport in NPC disease ameliorates liver dysfunction and neurodegeneration in the npc1-/- mouse. Proc Natl Acad Sci USA 2009;106:2377–2382.
46 Frank DW, Gray JE, Weaver RN. Cyclodextrin nephrosis in the rat. Am J Pathol 1976;83:367–382.
47 Schmid G. Preparation and application of γ-cyclodextrin. In: Duchene D, ed. New Trends in Cyclodextrins and Derivatives. Paris: Editions de Sante, 1991:27–54.
48 Arima H, Motoyama K, Irie T. Recent findings on safety profiles of cyclodextrins, cyclodextrin conjugates and polypseudorotaxanes. In: Bilensoy E, ed. Cyclodextrins in Pharmaceutics, Cosmetics and Biomedicine: Current and Future Industrial Applications. John Wiley & Sons, USA 2011:91–122.


See www.StemCells.com for supporting information available online.

Journal of Molecular Cell Biology Advance Access published July 3, 2014

doi:10.1093/jmcb/mju029 *Journal of Molecular Cell Biology* (2014), 0(0), 1–15 | 1

Article

Generation of insulin-producing β-like cells from human iPS cells in a defined and completely xeno-free culture system

Hussain Md. Shahjalal[1,2], Nobuaki Shiraki[1], Daisuke Sakano[1,2], Kazuhide Kikawa[1,2,3], Soichiro Ogaki[1], Hideo Baba[4], Kazuhiko Kume[5], and Shoen Kume[1,2,6,*]

[1] Department of Stem Cell Biology, Institute of Molecular Embryology and Genetics, Kumamoto University, Honjo 2-2-1, Chuo-Ku, Kumamoto 860-0811, Japan
[2] Global-Center of Excellence (G-COE), Kumamoto University, Honjo 2-2-1, Chuo-ku, Kumamoto 860-0811, Japan
[3] Department of Pediatrics, Graduate School of Medical Sciences, Kumamoto University, Honjo 1-1-1, Chuo-Ku, Kumamoto 860-8556, Japan
[4] Department of Gastroenterological Surgery, Graduate School of Medical Sciences, Kumamoto University, Honjo 1-1-1, Chuo-Ku, Kumamoto 860-8556, Japan
[5] Department of Neuropharmacology, Graduate School of Pharmaceutical Sciences, Nagoya City University, 3-1 Tanabe Street, Mizuho, Nagoya 467-8603, Japan
[6] Program for Leading Graduate Schools 'HIGO (Health Life Science; Interdisciplinary and Glocal Oriented) Program,' Kumamoto University, Honjo 2-2-1, Chuo-ku, Kumamoto 860-0811, Japan
* Correspondence to: Shoen Kume, E-mail: skume@kumamoto-u.ac.jp

Human induced pluripotent stem (hiPS) cells are considered a potential source for the generation of insulin-producing pancreatic β-cells because of their differentiation capacity. In this study, we have developed a five-step xeno-free culture system to efficiently differentiate hiPS cells into insulin-producing cells *in vitro*. We found that a high NOGGIN concentration is crucial for specifically inducing the differentiation first into pancreatic and duodenal homeobox-1 (PDX1)-positive pancreatic progenitors and then into neurogenin 3 (NGN3)-expressing pancreatic endocrine progenitors, while suppressing the differentiation into hepatic or intestinal cells. We also found that a combination of 3-isobutyl-1-methylxanthine (IBMX), exendin-4, and nicotinamide was important for the differentiation into insulin single-positive cells that expressed various pancreatic β-cell markers. Most notably, the differentiated cells contained endogenous C-peptide pools that were released in response to various insulin secretagogues and high levels of glucose. Therefore, our results demonstrate the feasibility of generating hiPS-derived pancreatic β-cells under xeno-free conditions and highlight their potential to treat patients with type 1 diabetes.

Keywords: diabetes, pancreas, cell therapy, hiPS cells, xeno-free differentiation, β-cells

Introduction

Diabetes is a life-long disease characterized by chronic hyperglycemia. Type 1 diabetes is caused by autoimmune destruction of insulin-producing β-cells in the pancreas and its treatment is solely dependent on insulin administration. Islet transplantation from cadaveric donors is a promising therapy for type 1 diabetes; however, due to difficulties such as the scarcity of cadaveric donors compared with the large number of diabetic patients, the low yield of transplantable islets from cadaveric pancreas, and the necessity of chronic immunosuppression (Shapiro et al., 2006; Shapiro, 2011), alternative cell sources for the generation of insulin expressing β-cells are needed.

Human pluripotent stem cells, e.g. human embryonic stem (hES) cells and human induced pluripotent stem (hiPS) cells, possess the capacity for unlimited replication and the potential to differentiate into all major somatic cell lineages (Thomson et al., 1998; Takahashi et al., 2007). Therefore, they have great potential for use in cell therapy and drug discovery. Many studies reported the generation of pancreatic endocrine cells (ECs) *in vitro* from hES/iPS cells in feeder-cell culture systems (D'Amour et al., 2006; Kroon et al., 2008; Chen et al., 2009; Kunisada et al., 2012) or feeder-free culture systems (Jiang et al., 2007a, b; Zhang et al., 2009; Rezania et al., 2012). Studies on the differentiation of hES or iPS cells into endodermal or pancreatic cell lineages have shown that activin A, fibroblast growth factor (FGF), stimulation with retinoic acid (RA), and inhibition of hedgehog, bone morphogenetic protein (BMP), and transforming growth factor (TGF)-β signaling promote the differentiation into endodermal or pancreatic lineages (D'Amour et al., 2006; Kroon et al., 2008; Chen et al., 2009; Mfopou et al., 2010; Kunisada et al., 2012; Rezania et al., 2012). Stepwise differentiation protocols were designed to mimic pancreatic differentiation and to successfully generate insulin

Received February 5, 2014. Revised April 28, 2014. Accepted May 14, 2014.

(INS)-expressing cells from hES or iPS cells. However, to date, pancreatic β-like cells generated from hES/iPS cells *in vitro* are largely polyhormonal and exhibit limited capacity of glucose-stimulated insulin secretion (GSIS), a characteristic of functionally mature β-cells (D'Amour et al., 2006; Chen et al., 2009; Zhang et al., 2009; Kunisada et al., 2012; Bruin et al., 2014). Moreover, most of the current differentiation protocols utilize a variety of undefined animal-derived products that may have unknown effects on cell characteristics and differentiation. The potential consequences of transplanting human cells exposed to animal-derived products into patients include an increased risk of graft rejection, immunoreactions, and microbial infections, prions, and yet unidentified zoonoses (Cobo et al., 2005; Martin et al., 2005; Skottman and Hovatta, 2006). Some reports describe protocols that involved the use of xeno-free components to generate pancreatic ECs from human pluripotent stem cells (Micallef et al., 2012; Schulz et al., 2012). Micallef et al. (2012) used xeno-free media; however, they also used mouse embryonic fibroblasts for passaging. Schulz et al. (2012) expanded hES cells in xeno-free media without feeder cells but they used fetal bovine serum during differentiation. Therefore, the establishment of a defined and completely xeno-free culture system with which functional and terminally differentiated endocrine cell types can be generated from hiPS cells is needed for future research and clinical applications.

To address these issues, we established for the first time a defined and completely xeno-free culture system to derive INS-expressing β-like cells from hiPS cells using a synthetic scaffold and serum-free media containing humanized and/or recombinant supplements and growth factors. We demonstrated that combined use of NOGGIN and 3-isobutyl-1-methylxanthine (IBMX) enhanced and directed hiPS-derived cells to differentiate into INS-expressing β-like cells. The differentiated cells secreted C-peptide *in vitro* in response to various insulin secretagogues and high glucose levels and expressed several pancreatic β-cell markers.

Results

Self-renewal and maintenance of undifferentiated hiPS cells under xeno-free conditions

We found that the levels of *N*-glycolylneuraminic acid (Neu5Gc), an indicator of xenogeneic contamination in human pluripotent stem cell cultures (Martin et al., 2005), markedly decreased to an undetectable level in hiPS cells grown under xeno-free conditions after passage 2 (P2) (Figure 1B). In addition, hiPS cells grown under xeno-free conditions (P3) maintained their self-renewal capacity and pluripotency, as confirmed by positive alkaline phosphatase staining and the expression levels of octamer-4 (OCT4), NANOG, SRY box-2 (SOX2), tumor rejection antigen 1-81 (TRA1-81), and stage-specific embryonic antigen-4 (SSEA-4), which were similar to those of hiPS cells grown under xenogeneic conditions (Supplementary Figure S1A). There was no detectable expression of stage-specific embryonic antigen-1 (SSEA-1), a marker associated with hES cell differentiation, suggesting that hiPS cells maintained the undifferentiated state under xeno-free conditions. HiPS cells grown under xeno-free conditions also exhibited a distinctive morphology of sharp-edged, flat, and tightly packed colony structures (Supplementary Figure S1B), characteristic of pluripotent stem cells. Therefore, our xeno-free system is effective for keeping hiPS cells free of contamination from non-human-derived factors, while maintaining their pluripotency.

Differentiation into pancreatic progenitor cells at high NOGGIN concentrations

We developed a five-step protocol for the differentiation of hiPS cells into pancreatic hormone-expressing cells under xeno-free conditions (Figure 2A) by optimizing the protocol in a stepwise fashion.

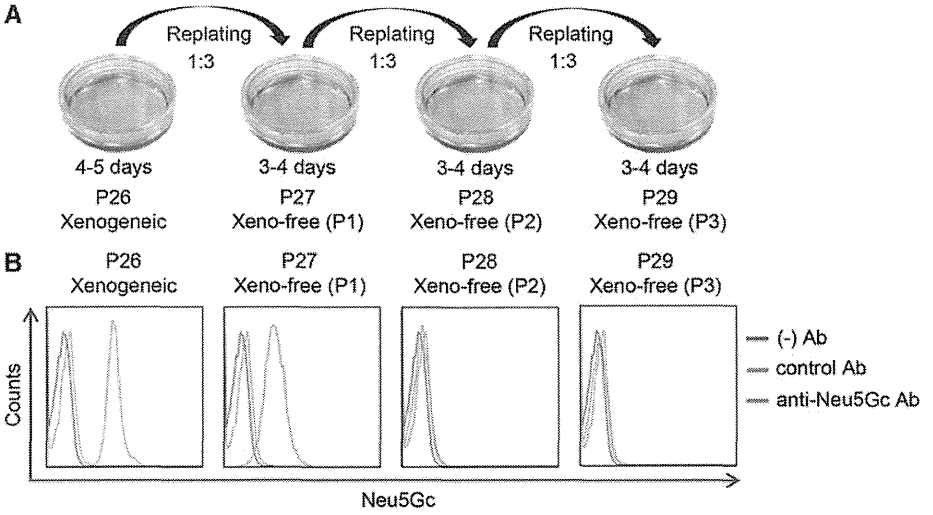

Figure 1 Maintenance of undifferentiated hiPS cells under xeno-free conditions. HiPS cells grown under xeno-free conditions showed a decreased expression of Neu5Gc after two passages. (**A**) Schematic drawing of the xeno-free culture system for proliferation and re-plating of undifferentiated hiPS cells. (**B**) The expression of Neu5Gc, a marker of xenoantigenic contamination, in undifferentiated hiPS cells grown under xenogeneic or xeno-free conditions by flow cytometry. Cells were exposed to an anti-Neu5Gc antibody (orange), a control antibody (blue), or incubated without a primary antibody (red), and then stained with a secondary antibody for analysis. P, passage; Ab, antibody.

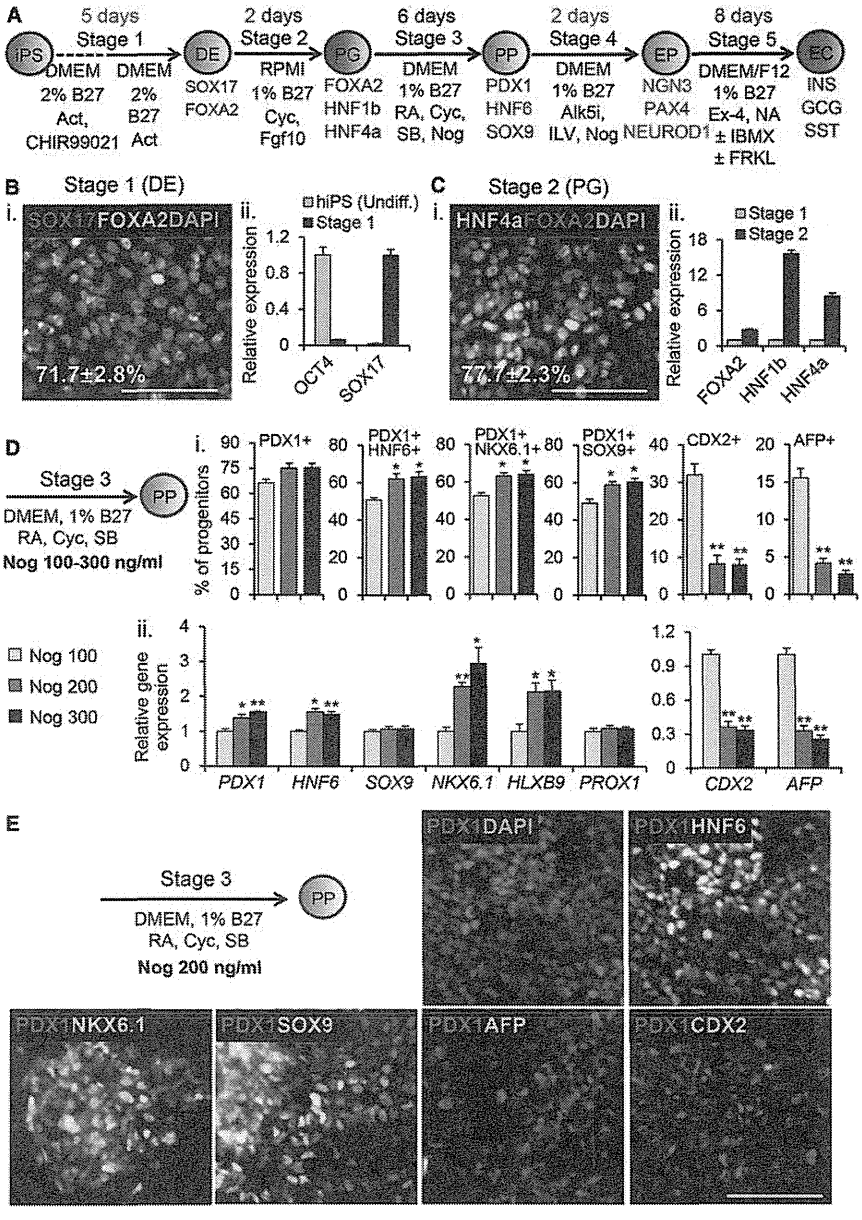

Figure 2 *In vitro* xeno-free differentiation of hiPS cells into DE, PG, and PP cells. The protocol was optimized to ensure hiPS cell differentiation into DE, PG, and PP cells. High concentrations of NOGGIN directed the differentiation into pancreatic lineages while suppressing differentiation into other lineages. (**A**) Schematic of the differentiation procedure into DE cells (stage 1), PG cells (stage 2), PP cells (stage 3), EP cells (stage 4), and ECs (stage 5). (**B**) SOX17/FOXA2-positive cells (i), and relative mRNA expression of DE markers (ii) at the end of stage 1. mRNA expression was compared with that of undifferentiated hiPS cells. (**C**) HNF4a/FOXA2-positive cells (i) and relative mRNA expression of PG markers (ii) at the end of stage 2. mRNA expression was compared with that of the stage-1 cells. (**D**) Percentages of PDX1-, PDX1/HNF6-, PDX1/NKX6.1-, PDX1/SOX9-, CDX2-, and AFP-positive cells generated with NOGGIN 100, 200, and 300 ng/ml (Nog 100, Nog 200, and Nog 300) (i), and relative mRNA expressions of pancreatic, intestinal, and hepatic progenitor markers (ii) at the end of stage 3. (**E**) Immunocytochemistry showing the expression patterns of PDX1- (red, pancreatic), HNF6- (green, pancreatic), NKX6.1- (green, pancreatic), SOX9- (green, pancreatic), CDX2- (green, intestinal), and AFP (green, hepatic)-positive cells generated with NOGGIN 200 ng/ml at stage 3. Cells were counterstained with DAPI (blue). The *glyceraldehyde-3-phosphate dehydrogenase* (*GAPDH*) transcript was used as internal RNA control. Results of both immunocytochemistry and quantitative RT–PCR are presented as mean ± SEM of three independent experiments ($n = 3$). Student's *t*-tests were performed against the values of Nog 100 or between two discrete data sets, $^{*}P < 0.05$, $^{**}P < 0.01$. Scale bar, 100 μm.